Dislocation-mediated melting in two dimensions

David R. Nelson and B. I. Halperin
Department of Physics, Harvard University, Cambridge, Massachusetts 02138
(Received 24 August 1978)

A theory of dislocation-mediated melting in two dimensions is described in detail, with an emphasis on results for triangular lattices on both smooth and periodic substrates. The transition from solid to liquid on a *smooth* substrate takes place in two steps with increasing temperatures. Dissociation of dislocation pairs first drives a transition out of a low-temperature solid phase, with algebraic decay of translational order and long-range orientational order. This transition is into a "liquid-crystal" phase characterized by exponential decay of translational order, but power-law decay of sixfold orientational order. Dissociation of *disclination* pairs at a higher temperature then produces an isotropic fluid. The behavior of the specific heat, structure factor, and various elastic constants near these transitions is worked out. We also discuss the applicability of our results to melting on a periodic substrate. Dislocation unbinding should describe melting of a "floating" (and, in general, incommensurate) adsorbate solid into a high-temperature fluid phase. The orientation bias imposed by the substrate can alter or eliminate the disclination-unbinding transition, however. Transitions from a floating solid into a *low*-temperature registered or partially registered phase can also be mapped onto the dislocation-unbinding transition, but only at certain special values of the coverage. Substrate reciprocal-lattice vectors play the role of Burger's vectors in this case.

I. INTRODUCTION

Building on ideas due to Kosterlitz and Thouless,[1] it has been possible to construct a reasonably detailed and complete theory of superfluidity on two dimensions.[2–5] One imagines a superfluid state in which phase fluctuations coexist with a dilute gas of bound vortex-antivortex pairs. The transition out of this state is assumed to be driven by the dissociation of a small fraction of these vortices. Calculations by José *et al.*[3] suggest that predictions of Kosterlitz[2] for a specific model Hamiltonian are, in fact, *universal* properties of $d=2$ superfluids and of related magnetic and liquid-crystal systems. A particularly striking result is that the superfluid density in a ^{4}He film should exhibit a universal jump discontinuity[4] at the critical temperature. This prediction, together with a theory of the dynamics of two-dimensional superfluidity at long wavelengths,[5] should ultimately allow detailed experimental tests of the theory.

Kosterlitz and Thouless have proposed that similar ideas apply to two-dimensional melting.[1] One now considers a "crystal" without conventional long-range order in which phonon excitations coexist with a dilute gas of bound dislocation pairs having equal and opposite Burger's vectors. The crystal melts at sufficiently high temperatures, driven by the dissociation of a small fraction of the pairs.

In a recent communication[6] we explored these ideas further and found that, in fact, a second disclination-unbinding transition is necessary to complete the transition from solid to liquid. We also discussed the applicability of the theory to melting on a periodic substrate. In this paper we present the details of our investigation. The ideas behind the theory, as well as the principal results, are summarized in Sec. I A and B.

A. Melting on a smooth substrate

We first discuss two-dimensional melting in the absence of a periodic substrate potential—melting on a smooth substrate. Consider the properties of a solid film on such a substrate. By a solid we mean a substance whose equilibrium behavior is describable by continuum elasticity theory[7] with nonzero long-wavelength elastic constants. Such a solid displays interesting properties[8] notwithstanding arguments by Peierls[9] and Landau[10] (and a rigorous proof by Mermin[11]) that true translational long-range order is impossible in such systems.

The absence of long-range order shows up clearly in the structure function, defined by

$$S(\vec{q}) = \langle |\hat{\rho}(\vec{q})|^2 \rangle \ , \tag{1.1a}$$

where $\hat{\rho}(\vec{q})$ is the Fourier transform of the density. In a solid phase, we can write

$$S(\vec{q}) = \sum_{\vec{R}} e^{i\vec{q}\cdot\vec{R}} \langle e^{i\vec{q}\cdot[\vec{u}(\vec{R})-\vec{u}(\vec{0})]} \rangle \ , \tag{1.1b}$$

where the summation is over the sites $\{\vec{R}\}$ of a triangular lattice, and the position of an individual atom in the solid is $\vec{r}=\vec{R}+\vec{u}(\vec{R})$. We shall focus most of our attention on melting of triangular lattices for reasons of simplicity (they can be described by an isotropic elastic tensor[7]) and because these are the most common regular structures in two dimensions.

In a three-dimensional solid the function $S(\vec{q})$ has a set of δ-function Bragg peaks, occurring at the reciprocal-lattice vectors $\{\vec{G}\}$ corresponding to the lattice of sites $\{\vec{R}\}$. The δ-function character of the Bragg peaks reflects the finiteness of the displacements $\vec{u}(\vec{R})$, which assures that the Debye-Waller correlation function $C_{\vec{G}}(\vec{R})$ tends to nonzero constant at large $\vec{R}$. Here, $C_{\vec{G}}$ is defined by

$$C_{\vec{G}}(\vec{R}) \equiv \langle \rho_{\vec{G}}(\vec{R}) \rho_{\vec{G}}^*(\vec{0}) \rangle \ , \tag{1.2}$$

$$\rho_{\vec{G}}(\vec{R}) \equiv e^{i\vec{G}\cdot[\vec{R}+\vec{u}(\vec{R})]} \ . \tag{1.3}$$

In two dimensions, however, it is known that the displacements $\vec{u}(\vec{R})$ diverge logarithmically due to fluctuations in the long-wavelength phonon modes, and that $C_{\vec{G}}(\vec{R})$ tends algebraically to zero at large $\vec{R}$,[8,12]

$$C_{\vec{G}}(\vec{R}) \sim R^{-\eta_{\vec{G}}(T)} \ . \tag{1.4}$$

The exponent $\eta_{\vec{G}}(T)$ is related to the Lamé elastic constants of the solid [which we denote $\mu_R(T)$ and $\lambda_R(T)$] by

$$\eta_{\vec{G}}(T) = k_B T |\vec{G}|^2 (3\mu_R + \lambda_R)/4\pi\mu_R(2\mu_R + \lambda_R) \ . \tag{1.5}$$

There is no translational long-range order; the expectation value of the translational order parameter $\rho_{\vec{G}}(\vec{R})$ must vanish in an infinite sample. Nevertheless, the slow power-law decay of $C_{\vec{G}}(\vec{R})$, given by Eq. (1.4), is very different from the exponential decay one would expect in a liquid. Inserting Eq. (1.4) into Eq. (1.1b), we find that power-law singularities[12] replace the δ-function Bragg peaks at a set of recirpocal-lattice vectors $\{\vec{G}\}$,

$$S(\vec{q}) \sim |\vec{q}-\vec{G}|^{-2+\eta_{\vec{G}}(T)} \ . \tag{1.6}$$

Since power-law behavior is usually associated with critical points,[13] we can in some sense regard a solid film as consisting of a phase of critical points with temperature-dependent critical indices $\{\eta_{\vec{G}}(T)\}$. Note that there is in general a different critical index associated with each Bragg position $\vec{G}$.

It is also convenient to consider an order parameter for bond orientations, which for triangular lattices is

$$\psi(\vec{r}) = e^{6i\theta(\vec{r})} \ , \tag{1.7}$$

where $\theta(\vec{r})$ is the orientation relative to some fixed reference axis of the bond between two neighboring atoms. [For a square lattice, the appropriate quantity would be $e^{4i\theta(\vec{r})}$]. In a solid film $\theta(\vec{r})$ defined modulo $\frac{1}{3}\pi$, is simply related to the displacement field $\vec{u}(\vec{r})$, i.e.,

$$\theta(\vec{r}) = \frac{1}{2}\left[\frac{\partial u_y(\vec{r})}{\partial x} - \frac{\partial u_x(\vec{r})}{\partial y}\right] \ . \tag{1.8}$$

The orientational correlation function $\langle \psi^*(\vec{r})\psi(\vec{0})\rangle$ approaches a constant for large $\vec{r}$ in a two-dimensional solid, as has been pointed out for a slightly different correlation function by Mermin.[11,14] Thus, a solid film displays long-range orientational order of the conventional sort. This may be contrasted with the exponential decay of orientational correlations we would expect in a liquid.

Kosterlitz and Thouless[1] argued that an unbinding of dislocation pairs at a temperature T_m would cause the solid described above to melt into a liquid. We find that a transition of this kind does occur, but that the new phase is actually a new type of liquid crystal. Above T_m a finite density of free dislocations $n_f(T)$ leads to exponentially decaying translational order,

$$C_{\vec{G}}(\vec{R}) \sim e^{-R/\xi_+(T)} \ , \tag{1.9}$$

with a correlation length that diverges as T approaches T_m from above, according to

$$\xi_+(T) \sim \exp(\text{const}/(T-T_m)^{\bar{\nu}}) \ , \tag{1.10a}$$

with[15]

$$\bar{\nu} = 0.36963\cdots \ . \tag{1.10b}$$

(An explicit expression for the number 0.36963··· is given in Sec. III.) We find, however, that orientational order persists above T_m, in the sense that bond angle correlations now decay *algebraically* to zero,

$$\langle \psi^*(\vec{r})\psi(\vec{0})\rangle \sim r^{-\eta_6(T)} \ . \tag{1.11}$$

A similar algebraic decay of orientational order is expected in a two-dimensional nematic liquid crystal[16,17] except that $\psi(\vec{r})$, for the nematic, is equal to $e^{2i\theta(\vec{r})}$, and $\theta(\vec{r})$, defined modulo 180°, is the orientation of the director field. In the present case of melting from a triangular lattice the liquid crystal has sixfold anisotropy, rather than the twofold anisotropy of the nematic. We expect that a square lattice would melt into a liquid crystal with fourfold anisotropy. We propose that these new phases be called "hexatic" and "tetratic" liquid crystals, respectively.

We find that the energy of a long-wavelength orientation fluctuation in this anisotropic fluid takes the form

$$\mathcal{H}_A = \tfrac{1}{2} K_A \int d^2r (\vec{\nabla}\theta)^2 \ , \tag{1.12}$$

where the Frank constant $K_A(T)$ diverges near T_m, i.e.,

$$K_A(T) \sim \xi_+^2(T) \ . \tag{1.13}$$

The exponent $\eta_6(T)$ is related to $K_A(T)$ by

$$\eta_6(T) = 18 k_B T/\pi K_A(T) \quad . \tag{1.14}$$

Below T_m, all dislocations are bound and their only effect on the properties of the solid film is to renormalize the Lamé constants which appear in the elastic energy. This energy takes the form,[7]

$$\mathcal{H}_0 = \tfrac{1}{2} \int d^2 r \,(2\mu_R u_{ij}^2 + \lambda_R u_{ii}^2) \quad , \tag{1.15a}$$

where $u_{ij}(\vec{r})$ is the strain tensor

$$u_{ij}(\vec{r}) = \frac{1}{2}\left[\frac{\partial u_i(\vec{r})}{\partial r_j} + \frac{\partial u_j(\vec{r})}{\partial r_i}\right] , \tag{1.15b}$$

and the elastic constants $\mu_R(T)$ and $\lambda_R(T)$ approach *finite* limiting values as $T \to T_m^-$. Just below T_m we find

$$\mu_R(T) = \mu_R(T_m^-)\,|1 + \text{const}(T_m - T)^{\bar{\nu}}| \quad , \tag{1.16}$$

with a similar expression for $\lambda_R(T)$. There is a universal relationship involving $\mu_R(T)$ and $\lambda_R(T)$ at the melting temperature

$$\lim_{T \to T_m^-} \left[\frac{1}{\mu_R(T)} + \frac{1}{\mu_R(T) + \lambda_R(T)}\right] = \frac{a_0^2}{4\pi k_B T_m} \quad , \tag{1.17}$$

where a_0 is the lattice spacing. The entropy argument of Kosterlitz and Thouless also leads to a result of this sort, which they suggested would hold as an inequality.[1] Power-law singularities in the structure factor of the form (1.6) persist right up to the melting temperature. Comparing Eqs. (1.17) and (1.5), we find that the values at T_c of the exponents $\eta_{\vec{G}}(T)$ become universal functions of the two-dimensional Poisson's ratio[18] $\sigma_R(T) \equiv \lambda_R/(\lambda_R + 2\mu_R)$, namely,

$$\eta_{\vec{G}}^* \equiv \lim_{T \to T_m^-} \eta_{\vec{G}}(T) = \frac{G^2 a_0^2}{64\pi^2} \lim_{T \to T_m^-} [1 + \sigma_R(T)][3 - \sigma_R(T)] \quad . \tag{1.18}$$

(Note that the combination Ga_0 is independent of the lattice constant for a Bragg point of given order.) Since $\sigma_R(T)$ cannot exceed unity, we obtain bounds on the exponents $\eta_{\vec{G}}^*$. The exponent $\eta_{\vec{G}_0}^*$ for the first Bragg point of a triangular lattice, for example, cannot exceed $\frac{1}{3}$. Above T_m the structure factor is finite at all Bragg positions and the Lamé coefficients vanish at long wavelengths. As T approaches T_m from above, $S(\vec{G})$ acquires a singular contribution

$$S(\vec{G}) \sim \xi_+(T)^{2-\eta_{\vec{G}}^*} \quad , \tag{1.19}$$

while the specific heat displays only an essential singularity

$$C_p(T) \sim \xi_+^{-2}(T) \quad . \tag{1.20}$$

Thus far, we have ignored the effect of disclinations. Bound states of these angular singularities exist even in the solid phase—an isolated dislocation can itself be regarded as a pair of disclinations a lattice spacing apart.[19] [An elementary dislocation on a triangular lattice and its construction out of a pair of disclinations is illustrated in Fig. 1(a). The corresponding construction for a square lattice, with disclinations a half lattice spacing apart, is shown in Fig. 1(b).] Although disclinations remain very tightly bound (in pairs with equal and opposite disclinicity) at all temperatures up to T_m, screening by a density $n_f(T) \approx \xi_+^{-2}(T)$ of free dislocations, produces a weaker logarithmic binding of disclinations for $T > T_m$.

We can now apply to the liquid-crystal phase the analysis which Kosterlitz and Thouless[1,2] used for two-dimensional superfluids. Bound pairs of $\pm 60°$

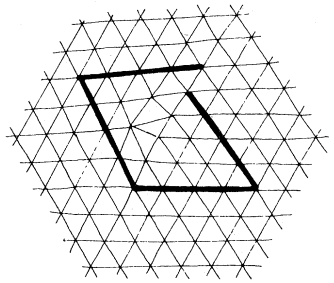

(a)

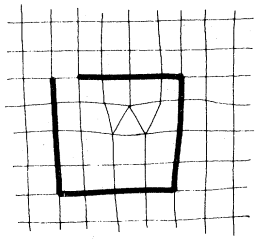

(b)

FIG. 1. (a) Elementary dislocation on a triangular lattice. The Burger's vector is the amount by which the path around the singularity fails to close. The path would be a closed circuit on a perfect lattice. Note that the dislocation can be viewed as seven- and five-coordinated disclinations one lattice-spacing apart. This figure is from a molecular-dynamics simulation by R. Morf. (b) Elementary dislocation on a square lattice. This can be viewed as a lattice point with five-fold symmetry and an interstitial point with three-fold symmetry separated by about half-a-lattice constant.

disclinations now play the role of bound vortex pairs. Eventually the algebraic decay of orientational order is converted to an exponential decrease by the dissociation of these disclination pairs at a second transition temperature $T_i > T_m$. Precisely at T_i, we find[2]

$$\eta_6(T_i) = \tfrac{1}{4} \quad . \tag{1.21}$$

The results Kosterlitz[2] obtained for the superfluid can be applied to the specific heat and orientational correlation length as well. Above T_i both translational and orientational order decay exponentially, and we have a conventional isotropic fluid phase.

The sequence of transitions which follow from our analysis of dislocation-mediated melting on a smooth substrate is illustrated in Fig. 2(a). Although the theory that leads to these results is stable and self-consistent, we cannot rule out the possibility of a first-order melting transition. Such a transition might be driven by a premature dissociation of disclination pairs, before dislocations dissociate.[20] Such a transition would be directly into a liquid phase, since loss of translational order must accompany loss of orientational order.

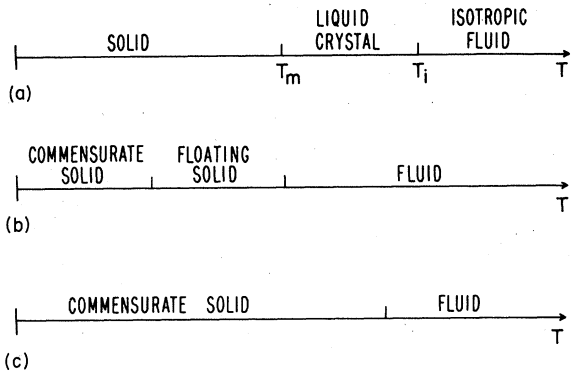

FIG. 2. Transition sequences for melting on smooth and periodic substrates. (a) On a smooth substrate, a low-temperature solid with long-range orientational order and algebraic decay of translational order is separated from an hexatic liquid crystal with algebraic decay of sixfold orientational order and exponentially decaying translational order by a dislocation-unbinding temperature T_m. A disclination unbinding at temperature T_i causes a transition into an isotropic fluid phase, where both orientational and translational correlations fall off exponentially. (b) In the presence of a very fine mesh commensurate substrate potential, a commensurate solid exists at low temperatures. The substrate is relatively unimportant in solid and fluid phases at higher temperatures. The disclination-unbinding transition which would occur in the fluid on a smooth substrate is altered or eliminated, however. (c) If the substrate mesh is too coarse, only commensurate solid and fluid phases occur.

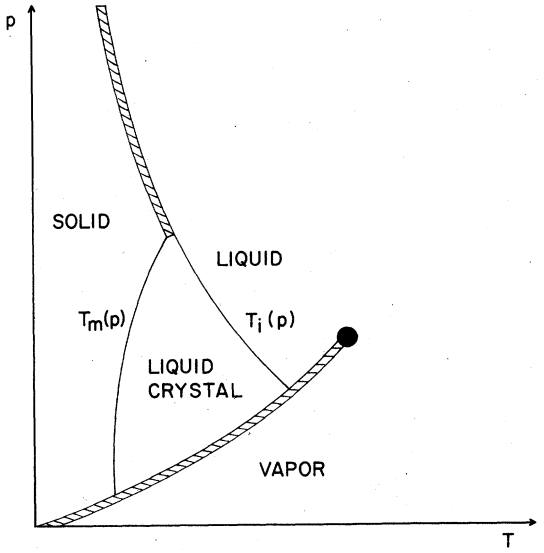

FIG. 3. Solid, liquid, vapor, and hexatic liquid-crystal phases in a speculative pressure-temperature phase diagram for circularly symmetric molecules with an attractive potential. Hatched lines indicate first-order transitions.

A possible temperature-pressure phase diagram for circularly symmetric molecules with an attractive potential is shown in Fig. 3. Both two-stage solid-liquid transitions [at temperatures $T_m(p)$ and $T_i(p)$] and first-order melting transitions are shown. The line of first-order transitions at high pressures would be consistent with computer simulations by Alder and Wainwright[21] of hard-disk melting. It should be emphasized, however, that many other phase diagrams are possible, with or without regimes of two-stage second-order melting transitions.

Several two-dimensional systems exist which could conceivably be described by a theory of melting on a smooth substrate. The first of these are thin "soap-bubble" films of smectic-B or -H liquid crystals.[22] In particular, the theory may be applicable to the transition from a smectic-B to a smectic-A film. Birgeneau and Litster[23] have gone further and have suggested that the bulk smectic-B phase may be understood as a three-dimensional generalization of the hexatic-liquid-crystal phase, in which there is long-range orientational order with a sixfold anisotropy axis perpendicular to the smectic layers and short-range translational order in the planes. Indeed, if one were to build a three-dimensional material out of hexatic-liquid-crystal layers and if the coupling between the layers was very weak, one would expect an equilibrium state with just these features. If this analogy is correct, then smectic-B to smectic-A transition in a film would be an example of the disclination-unbinding transition discussed in this paper.

An interesting experimental system, where a solid-

liquid transition is expected to occur, is the system of electrons trapped on the surface of liquid helium.[24] Thouless has discussed application of the dislocation-unbinding transition to this system.[25] The arguments presented in this paper would lead one to expect a higher temperature disclination unbinding transition as well.

B. Melting on a periodic substrate

Because a large number of experimental investigations of two-dimensional melting are carried out on films epitaxially adsorbed[26] onto a periodic substrate, it is important to determine the effect of a periodic potential on the theory sketched in Sec. I A.

A possible adsorbate-phase diagram is shown in Fig. 4. Because of the substrate potential, one must now distinguish between "commensurate" and "floating" solid phases. In a commensurate solid an adsorbate lattice or superlattice is locked to the substrate periodicity. (Three commensurate phases are shown in Fig. 4 together with floating solid and fluid phases.) Mathematically we expect a commensurate solid to have δ-function Bragg peaks at a lattice of vectors, which includes the two-dimensional reciprocal lattice $\{\mathbf{K}\}$ of the substrate surface as a proper subset. A floating solid, on the other hand, is characterized by power-law Bragg singularities at a set of reciprocal-lattice vectors $\{\mathbf{G}\}$, which vary continuously with coverage and temperature; δ-function Bragg peaks at substrate reciprocal-lattice points $\{\vec{\mathbf{K}}\}$ should be present as well. The phases called commensurate solids in this paper were referred to as epitaxial solids in Ref. 6.

Note that we do not require *every* atom to be in registry in what we call a commensurate solid.

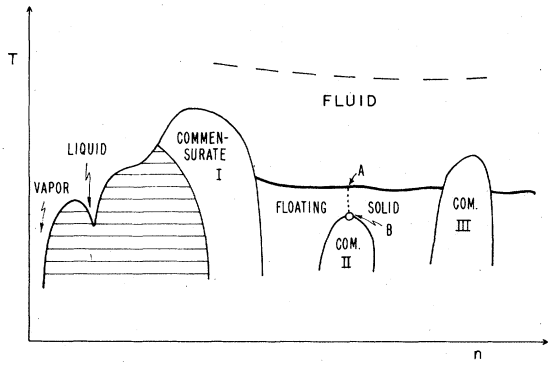

FIG. 4. Schematic adsorbate phase diagram as a function of density and temperature at submonolayer densities. Fluid, floating solid, and various commensurate phases are shown. The dashed line indicates a Ising-like phase transition, separating fluid phases with different orientational symmetry. Such a line would be absent for a triangular substrate, but could occur for substrates with a square symmetry.

Although a phase with only a superlattice of adsorbed atoms locked to the substrate might better be called partially commensurate, we prefer not to distinguish between partial and complete registry. Also, the phase we call a floating solid is often termed an "incommensurate solid" in the literature. We prefer our designation, because we wish to discuss a situation where a floating solid is accidentally commensurate with the substrate, at a particular coverage and temperature. A locus of such commensurate points in the solid phase is represented by the dotted line in Fig. 4. In the literature, there has been a distinction between an epitaxial fluid, which has an average interparticle separation close to one preferred by the substrate, and a fluid in which the substrate plays a less important role.[27] Because it seems unlikely to us that such fluids are separated by sharp phase boundaries, we do not make this distinction and choose to call the entire high-temperature region of Fig. 4(a) fluid (the dashed line will be explained later). Two-phase coexistence is shown between liquid and vapor phases of this fluid, although this need not always be the case.[28] Another region of two-phase coexistence separates commensurate phase I from the dilute fluid or vapor.[26,28] As an example, commensurate phase I may represent something like the $\sqrt{3}\times\sqrt{3}$ registered structure of krypton adsorbed on graphite.

The heavy line separating the floating solid and fluid phases represents a dislocation unbinding very similar to that which would occur on a smooth substrate. The predictions for the structure factor, elastic constants, and specific heat are the same as for a smooth substrate, except that the exponent $\bar{\nu}$ entering Eqs. (1.10) and (1.16) must be replaced by a substrate-dependent result. Because the adsorbate lattice is locked into a preferred orientation relative to the substrate, an additional term $2\gamma_R \int d^2r\, \theta^2(\vec{r})$ appears in Eq. (1.15) with θ given by Eq. (1.8). The new elastic constant γ_R measures the energy associated with local deviations from perfect alignment. The universal relation between μ_R, λ_R, and γ_R at the melting temperature analogous to Eq. (1.17), is

$$\lim_{T\to T_m^-}\left[\frac{\mu_R(T)[\mu_R(T)+\lambda_R(T)]}{2\mu_R(T)+\lambda_R(T)}+\frac{\mu_R(T)\gamma_R(T)}{\mu_R(T)+\gamma_R(T)}\right]=\frac{4\pi k_B T_m}{a_0^2}\ , \quad (1.22)$$

where a_0 is the average adsorbate lattice spacing as seen, for example, in a neutron scattering experiment.

In general, one expects an increasing multiplicity and complexity of registered and partially registered phases with decreasing temperatures. One of our principal results is a criterion which determines whether or not a particular commensurate phase pierces the floating solid-fluid transition line. Analyzing the stability of a floating solid to a weak commen-

surate substrate potential, we find that *all* such perturbations lead to the formation of commensurate solids at sufficiently low temperatures. If the mesh of the substrate lattice is sufficiently fine relative to the commensurate super lattice mesh, such perturbations become unimportant at higher temperatures, before dislocations can unbind and destabilize the floating solid. The dotted line in Fig. 4 marks a locus of this kind, where the floating solid is stable to both perturbations tending to produce commensurate phase II and to dislocation unbinding. If the substrate mesh is too coarse relative to the commensurate superlattice, the periodic perturbation remains important out to quite high temperatures. There is then a transition directly from a commensurate phase into a fluid. This is the case for commensurate phase I and III. These two possible transition sequences are summarized in Figs. 2(b) and 2(c).

The precise criterion which differentiates between the phases can be stated as follows. Let $\vec{M}$ be the minimum nonzero reciprocal-lattice vector common to the two sets $\{\vec{G}\}$ and $\}\vec{K}\}$, of the adsorbate and substrate reciprocal lattices, respectively. We find that the renormalization-group eigenvalue[29] of the commensurate substrate potential in the floating solid phase is simply given by

$$\lambda_M(T) = 2 - \tfrac{1}{2}\eta_{\vec{M}}(T) \ ,$$

where $\eta_{\vec{M}}(T)$ is given by Eq. (1.5) with the replacements $\mu_R \to \mu_R + \gamma_R$ and $\lambda_R \to \lambda_R - 2\gamma_R$. This eigenvalue must be negative for the floating solid to be stable. A minimum requirement for a floating solid to exist is that $\lambda_M(T)$ become negative at temperature below the dislocation-unbinding temperature. Making use of Eq. (1.22), we are lead to the requirement

$$\frac{M^2}{G_0^2} > \frac{12(\mu_R+\gamma_R)^2(2\mu_R+\gamma_R)^2}{\mu_R(\mu_R^2+\lambda_R\mu_R+3\mu_R\gamma_R+2\lambda_R\gamma_R)(3\mu_R+\lambda_R+\gamma_R)} \ , \tag{1.23}$$

where $G_0 = 4\pi/(3)^{1/2}a_0$ is the minimum adsorbate reciprocal-lattice vector, and μ_R, λ_R, and γ_R are the limiting values of these elastic constants at T_m. In the limit of small γ and taking a Poisson's ratio of $\sigma_R = 0.6$, we find the requirement $M/G_0 \gtrsim 3.54$.

Although we are more limited in our ability to analyze commensurate-floating solid transitions, it is possible to treat this transition at the special point marked B, which is the lower end of the line where the floating solid has the same periodicity as the commensurate phase. This transition will occur at a temperature T_B such that $\lambda_M(T_B) = 0$. In Sec. V we demonstrate that this transition is closely related to the transition at T_A; something which can be described mathematically as a dislocation unbinding occurs with decreasing temperatures, where substrate reciprocal-lattice vectors play the role of Burger's vectors.

The fluid phase above the floating solid-fluid transition line is analogous to the liquid-crystal phase discussed in Sec. I A, except that the substrate induces long-range orientational order. If the substrate and adsorbate lattices both have sixfold orientational symmetry, then the substrate couples linearly to the orientational order parameter ψ and orientational order tends gradually to zero with increasing temperatures. Thus, the disclination-unbinding transition (indicated by the dashed line of Fig. 4) is smeared out by the substrate potential and does not really exist as a sharp transition. For square substrate and triangular adsorbate lattices, however, we find that the disclination unbinding is converted into a sharp Ising-like phase transition. This would presumably show up as a logarithmic specific heat anomaly along the dashed line. The applitude of the divergent part of such a specific heat could be quite small, however. Similar arguments would lead one to expect a Potts transition for nematiclike molecules after melting from a floating solid on a triangular substrate.

A salient physical feature of dislocation-mediated melting transitions in real systems, is that they are hard to see. The specific heat exhibits a virtually undetectable singularity, although there may be a maximum near T_m. Even the changes in the structure factor are not as dramatic as one might hope. Little evidence for a sharp transition has in fact been seen in specific-heat measurements[30] or in neutron scattering experiments[31] on the floating-solid-fluid transitions. The predicted discontinuities in the elastic constants at T_m are rather striking. It is important to remember, however, that only the $q = 0$ constants are actually discontinuous. The renormalized shear modulus at finite wave vectors $\mu_R(q,T)$, for example, is continuous through T_m. This is why the only reflection of the jump discontinuity of $\mu_R(0,T)$ in the specific heat is an essential singularity.

C. Relation to previous work

As we shall see, melting problems on both smooth and periodic substrates can be represented by a set of elastic degrees of freedom, together with a system of interacting dislocations, whose Hamiltonian is

$$\frac{\mathcal{H}_D}{k_B T} = \frac{-1}{8\pi} \sum_{\vec{r}\neq\vec{r}'} \left[K_1 \vec{b}(\vec{r}) \cdot \vec{b}(\vec{r}') \ln\left(\frac{|\vec{r}-\vec{r}'|}{a} \right) - K_2 \frac{\vec{b}(\vec{r}) \cdot (\vec{r}-\vec{r}') \vec{b}(\vec{r}') \cdot (\vec{r}-\vec{r}')}{|\vec{r}-\vec{r}'|^2} \right] + \frac{E_c}{k_B T} \sum_{\vec{r}} |\vec{b}(\vec{r})|^2 \ . \quad (1.24)$$

The $\{\vec{b}(\vec{r})\}$ are dimensionless Burger's vectors of the form $\vec{b}(\vec{r}) = m(\vec{r})\vec{e}_1 + n(\vec{r})\vec{e}_2$, where $m(\vec{r})$ and $n(\vec{r})$ are integers, and $\vec{e}_1$ and $\vec{e}_2$ are unit vectors spanning an underlying Bravais lattice. The couplings K_1 and K_2 are related to the elastic constants and are inversely proportional to temperature; E_c can be regarded as the core energy of a dislocation. The quantity a is a cutoff which we take to be the dislocation core diameter. For melting of triangular lattices on a smooth substrate we have $K_1 = K_2$. A Hamiltonian of this form (with $|K_2| \leq K_1$) also describes the transition from floating solid to commensurate phase II in Fig. 4 at the special point B.

One of us[32] has studied the properties of $\mathcal{H}_D$ for the special case $K_2 = 0$ in some detail. In this work a series of duality transformation was used to relate this simplified melting problem to Hamiltonians with short-ranged interactions more suitable for an approximate renormalization-group recursion analysis. Using both approximate and analytic renormalization techniques, it was found that the dislocation degrees of freedom were unimportant at low temperatures (large K_1) and that a dislocation-unbinding transition was controlled by the terminus of a stable surface of fixed points parametrized by K_1 and $\vec{e}_1 \cdot \vec{e}_2$. It was also shown that addition of the angular terms in Eq. (1.24) represent a marginal perturbation everywhere on this fixed surface. Thus, in general, a three-dimensional volume of fixed points is needed to describe the behavior of Eq. (1.24) near T_m, in complete generality. The possibility of disclination unbinding was not considered in Ref. 32.

In Sec. II and III, we restrict ourselves to triangular lattices ($\vec{e}_1 \cdot \vec{e}_2 = \frac{1}{2}$) and extend this treatment to the special case $K_1 = K_2$. Although this is all that is necessary to treat melting of triangular lattices on a smooth substrate, the more general Hamiltonian with $K_1 \neq K_2$ is necessary to describe melting on a periodic substrate. The recursion relations appropriate to this more general problem have recently been constructed by A. P. Young.[15]

In Sec. II we determine the renormalization-group equations which describe the solid below and near T_m. The behavior of the elastic constants, correlation length, specific heat, and structure factor in this region are derived in Sec. III. The properties of the orientational order parameter and disclination-unbinding transition are determined in Sec. IV. Melting in the presence of weak, strong, commensurate, and incommensurate substrate potentials is discussed in Sec. V.

II. RECURSION RELATIONS NEAR T_m ON A SMOOTH SUBSTRATE

A. Dislocation contribution to the elastic constants

The calculations in Ref. 32 were carried out on the reduced elastic Hamiltonian

$$\bar{\mathcal{H}}_E \equiv \frac{-\mathcal{H}_E}{k_B T} = -\frac{1}{2} \int \frac{d^2 r}{a_0^2} (2\bar{\mu} u_{ij}^2 + \bar{\lambda} u_{kk}^2) \ , \quad (2.1)$$

where $\bar{\mu}$ and $\bar{\lambda}$ are the usual Lamé coefficients divided by $k_B T$ and multiplied by the squared lattice spacing a_0 of the underlying lattice, i.e.,

$$\bar{\mu} = \mu a_0^2 / k_B T \ , \quad \bar{\lambda} = \lambda a_0^2 / k_B T \ , \quad (2.2)$$

and the strain tensor $u_{ij}(\vec{r})$ is related to a displacement field $\vec{u}(\vec{r})$,

$$u_{ij}(\vec{r}) = \frac{1}{2} \left(\frac{\partial u_i(\vec{r})}{\partial r_j} + \frac{\partial u_j(\vec{r})}{\partial r_i} \right) \ . \quad (2.3)$$

The field $u_{ij}(\vec{r})$ contains a part

$$\phi_{ij}(\vec{r}) \equiv \frac{1}{2} \left(\frac{\partial \phi_i(\vec{r})}{\partial r_j} + \frac{\partial \phi_j(\vec{r})}{\partial r_i} \right)$$

due to smoothly varying complexions and a singular part $u_{ij}^{\text{sing}}(\vec{r})$ due to dislocations

$$u_{ij}(\vec{r}) = \phi_{ij}(\vec{r}) + u_{ij}^{\text{sing}}(\vec{r}) \ . \quad (2.4)$$

A dislocation located at site $\vec{r}$ is conveniently characterized by the amount by which a contour integral of the displacement field taken around it fails to close, i.e.,

$$\oint d\vec{u} = a_0 \vec{b}(\vec{r}) = n(\vec{r}) a_0 \vec{e}_1 + m(\vec{r}) a_0 \vec{e}_2 \ , \quad (2.5)$$

where $\vec{b}(\vec{r})$ is the dimensionless Burger's vector[19] associated with the singularity, and $n(\vec{r})$ and $m(\vec{r})$ are integers. The basis vectors $\vec{e}_1$ and $\vec{e}_2$ span an underlying square or triangular lattice.

Making use of results from continuum-elasticity theory[19] reviewed in Refs. 7 and 32, the singular part of the strain can be written

$$u_{ij}^{\text{sing}}(\vec{r}) = \left[\frac{1}{2\mu} \epsilon_{ik} \epsilon_{jl} \frac{\partial^2}{\partial r_k \partial r_l} - \frac{\lambda \delta_{ij}}{4\mu(\lambda+\mu)} \nabla^2 \right] \times a_0 \sum_{\vec{r}'} b_m(\vec{r}') \tilde{G}_m(\vec{r}, \vec{r}') \ , \quad (2.6)$$

where ϵ_{ij} is an antisymmetric 2×2 matrix,

$$\epsilon_{ij}=\begin{pmatrix}0 & 1\\ -1 & 0\end{pmatrix} .$$

The summation is over a square mesh of lattice sites with spacing a, which we take to be a dislocation core diameter. This lattice is merely a convenient way to introduce a cutoff and bears no relation to the underlying physical lattice which determines the value of the Burger's vectors. The Green's function $\tilde{G}_m(\vec{r})$ satisfies the equation

$$\nabla^4\tilde{G}_m(\vec{r},\vec{r}')=-K_0\epsilon_{mn}\frac{\partial}{\partial r_n}\delta(\vec{r}-\vec{r}') \tag{2.7}$$

with

$$K_0=4\mu(\mu+\lambda)/(2\mu+\lambda) . \tag{2.8}$$

For a crystal with free boundaries, the normal component of the stress must vanish at the edges, which leads to the boundary condition that $\vec{\nabla}G_m(\vec{r},\vec{r}')$ be a constant for all points $\vec{r}$ on the boundary. For $|\vec{r}-\vec{r}'|$ large compared to the lattice spacing, but far from the boundaries, we have

$$\begin{aligned}\tilde{G}_m(\vec{r},\vec{r}') &\approx \tilde{G}_m(\vec{r}-\vec{r}')\\ &=(-K_0/4\pi)\epsilon_{mn}(r_n-r_n')[\ln(|\vec{r}-\vec{r}'|/a)+C] .\end{aligned} \tag{2.9}$$

The positive constant C is a measure of the ratio of the dislocation core diameter to the lattice spacing. It is convenient to absorb C into an effective core energy (see below) and to take a to be the core diameter. Note that a need not be the same as a_0.

When the decomposition (2.4) is inserted into Eq. (2.1), the Hamiltonian breaks into two parts

$$\mathcal{H}_E=\mathcal{H}_0+\mathcal{H}_D , \tag{2.10}$$

where we have

$$\frac{\mathcal{H}_0}{k_BT}=\frac{1}{2}\int\frac{d^2r}{a_0^2}(2\bar{\mu}\phi_{ij}^2+\bar{\lambda}\phi_{kk}^2) .$$

A convenient alternative representation of $\mathcal{H}_0$ in terms of the vector field $\vec{\phi}$, provided boundary effects can be neglected, is

$$\frac{\mathcal{H}_0}{k_BT}=\frac{1}{2}\int\frac{d^2r}{a_0^2}[\bar{\mu}(\vec{\nabla}\vec{\phi})^2+(\bar{\mu}+\bar{\lambda})(\vec{\nabla}\cdot\vec{\phi})^2] , \tag{2.11}$$

where $(\vec{\nabla}\vec{\phi})^2\equiv(\partial_i\phi_j)^2$, and the summation convention is used. As shown in detail, for example, in Ref. 32, the dislocation part $\mathcal{H}_D$ takes the form[19]

$$\begin{aligned}\frac{\mathcal{H}_D}{k_BT}=\frac{-K}{8\pi}\sum_{\vec{r}\neq\vec{r}'}\Bigg[\vec{b}(\vec{r})\cdot\vec{b}(\vec{r}')\ln\left(\frac{|\vec{r}-\vec{r}'|}{a}\right)\\ -\frac{\vec{b}(\vec{r})\cdot(\vec{r}-\vec{r}')\,\vec{b}(\vec{r}')\cdot(\vec{r}-\vec{r}')}{|\vec{r}-\vec{r}|^2}\Bigg]\\ +\frac{E_c}{k_BT}\sum_{\vec{r}}|\vec{b}(\vec{r})|^2 ,\end{aligned} \tag{2.12}$$

where

$$K=K_0a_0^2/k_BT , \tag{2.13}$$

$$E_c=(C+1)Kk_BT/8\pi , \tag{2.14}$$

and a given complexion of Burger's vectors, must satisfy the constraint $\sum_{\vec{r}}\vec{b}(\vec{r})=0$. Note that Eq. (2.12) is the same as Eq. (1.24) with $K_1=K_2$.[33]

The calculations in Ref. 32 focused on the properties of $\mathcal{H}_D$, neglecting the dot product or angular terms in Eq. (2.12). Here we examine the renormalization of the elastic constants in Eq. (2.11) by the dislocation degrees of freedom. The calculations also provide a convenient way to incorporate the angular terms into the renormalization-group analysis presented in Ref. 32. The approach is similar in spirit to that used by Nelson and Kosterlitz[4] in calculating the superfluid density of a ^{4}He film.

The dislocation-free Hamiltonian $\mathcal{H}_0$ can be rewritten in the form

$$\frac{\mathcal{H}_0}{k_BT}=\frac{1}{2}\int\frac{d^2r}{a_0^2}\phi_{ij}C_{ijkl}\phi_{kl} , \tag{2.15}$$

where the tensor of bare elastic constants is just

$$C_{ijkl}=\bar{\mu}(\delta_{ik}\delta_{jl}+\delta_{il}\delta_{jk})+\bar{\lambda}\delta_{ij}\delta_{kl} . \tag{2.16}$$

The inverse of the tensor of renormalized elastic constants $C_{R,ijkl}^{-1}$, can be expressed in terms of a correlation function

$$C_{R,ijkl}^{-1}=\langle U_{ij}U_{kl}\rangle/\Omega a_0^2 , \tag{2.17}$$

where Ω is the area and

$$U_{ij}=-\tfrac{1}{2}\int_P(u_in_j+u_jn_i)dl . \tag{2.18}$$

The integration in Eq. (2.18) is over the perimeter P of the solid and $\vec{n}$ is a unit vector normal to this boundary. Equation (2.17) is readily derived by considering the response of $\langle U_{ij}\rangle$ to an infinitesimal external stress, treating each component of U_{ij} as an independent fluctuating variable. Although this last assumption is correct for a crystal subject to free-boundary conditions, it is not correct for the finite $\vec{k}$ Fourier components of $u_{ij}(\vec{r})$

$$\hat{u}_{ij}(\vec{k}) = \int d^2r\, e^{i\vec{k}\cdot\vec{r}} u_{ij}(\vec{r}) \quad , \tag{2.19}$$

which have only two independent components.[34] Consequently, $C^{-1}_{R,ijkl}$ is *not* simply given by

$$\lim_{\vec{k}\to 0} \frac{1}{\Omega} \langle \hat{u}_{ij}(\vec{k})\, \hat{u}_{kl}(-\vec{k}) \rangle \tag{2.20}$$

as one might expect.

Equation (2.17) is convenient for our purposes because the dislocation contribution to $C^{-1}_{R,ijkl}$ appears in a particularly simple form. Inserting the decomposition (2.4), we have

$$C^{-1}_{R,ijkl} = C^{-1}_{ijkl} + \Omega^{-1} \langle U^{\text{sing}}_{ij} U^{\text{sing}}_{kl} \rangle \quad , \tag{2.21}$$

where U^{sing}_{ij} is the dislocation contribution to U_{ij}, and where C^{-1}_{ijkl} is the inverse of the bare elasticity tensor (2.15)

$$C^{-1}_{ijkl} = \frac{1}{\Omega a_0^2} \left\langle \int d^2r_1\, \phi_{ij}(\vec{r}_1) \int d^2r_2\, \phi_{kl}(\vec{r}_2) \right\rangle$$

$$= \frac{1}{4\bar{\mu}} (\delta_{ik}\delta_{jl} + \delta_{il}\delta_{jk}) - \frac{\bar{\lambda}}{4\bar{\mu}(\bar{\mu}+\bar{\lambda})} \delta_{ij}\delta_{kl} \quad . \tag{2.22}$$

The tensor C^{-1}_{ijkl} is the inverse of C_{ijkl} in the sense that $C_{ijkl} C^{-1}_{klmn} = \frac{1}{2}(\delta_{im}\delta_{jn} + \delta_{in}\delta_{jm})$.

Although it is tempting to apply Green's theorem to Eq. (2.18) and obtain

$$U_{ij} = \int d^2r\, u_{ij}(\vec{r}) \quad ,$$

this is incorrect in the presence of dislocations, which make $\vec{u}(\vec{r})$ a multiple-valued function of $\vec{r}$. We may eliminate the multivaluedness by introducing a cut along the line segment joining each dislocation to the origin and requiring $\vec{u}$ to be continuous everywhere except on the cuts. The discontinuity in $\vec{u}$ at each cut is just the Burger's vector of the dislocation attached to the cut. If we now apply Green's theorem to Eq. (2.18), we find that

$$U_{ij} = \int d^2r\, u_{ij}(\vec{r}) + \sum_{\vec{R}} \tfrac{1}{2} a_0 \left[b_i(\vec{R})\, \epsilon_{jk} R_k + b_j(\vec{R})\, \epsilon_{ik} R_k \right] \quad , \tag{2.23}$$

where the second term is the contribution of the cuts. Equation (2.6), together with the requirement that $\vec{\nabla}\tilde{G}_m(\vec{r},\vec{r}')$ be constant on the boundary of the crystal, implies that the dislocation contribution to the first term in Eq. (2.23) vanishes so that the dislocation contribution to U_{ij} is simply

$$U^{\text{sing}}_{ij} = \tfrac{1}{2} a_0 \sum_{\vec{R}} \left[b_i(\vec{R})\, \epsilon_{jl} R_l + b_j(\vec{R})\, \epsilon_{il} R_l \right] \quad . \tag{2.24}$$

To check Eq. (2.24), consider the work done by a uniform external stress σ_{ij} when a pair of dislocations with equal and opposite Burger's vectors is moved to a separation $\vec{R}$. Since the force on the Burger's vector $\vec{b}$ due to a stress σ_{ij} is[19]

$$F_i = a_0 b_k \sigma_{kj} \epsilon_{ji} \quad , \tag{2.25}$$

(this is the analogue of the Magnus force on a vortex[35]) the work done is

$$\Delta W = a_0 b_k \epsilon_{ji} R_i \sigma_{kj} = \tfrac{1}{2} a_0 (b_k \epsilon_{ji} R_i + b_j \epsilon_{ki} R_i)\, \sigma_{kj} \quad . \tag{2.26}$$

However, this energy must also be given by the stress times the strain

$$\Delta W = \sigma_{ij} U^{\text{sing}}_{ij} \quad . \tag{2.27}$$

Comparing Eqs. (2.26) and (2.27), it follows immediately that:

$$U^{\text{sing}}_{ij} = \tfrac{1}{2} a_0 (b_i \epsilon_{jk} R_k + b_j \epsilon_{ik} R_k) \quad , \tag{2.28}$$

which agrees with Eq. (2.24) for two equal and opposite Burger's vectors at separation $\vec{R}$.

B. Recursion relations

In principle, the dislocation contribution to the elastic constants can now be determined as a power series in $y = e^{-E_c/k_B T}$. One need consider only configurations of two Burger's vectors to obtain results correct to $O(y^2)$ and so forth. We shall see, however, that such series become badly behaved as T approaches a temperature T_m which we identify with the melting transition. The series can be analyzed using a renormalization procedure which produces recursion relations for the elastic constants, and for K and y.

Two distinct complexions of Burger's vectors associated with a square lattice of excitations are shown in Fig. 5(a). These dislocations occur in pairs located at $\vec{r}_1$ and $\vec{r}_2$ with Burger's vectors $\pm\vec{e}_p$ with $p = 1, 2$, i.e.,

$$\vec{e}_1 = \begin{pmatrix} 1 \\ 0 \end{pmatrix}, \quad \vec{e}_2 = \begin{pmatrix} 0 \\ 1 \end{pmatrix} \quad . \tag{2.29}$$

The contribution to U^{sing}_{ij} of the pth pair is

$$\tfrac{1}{2} a_0 (e_{p,i}\epsilon_{jl} + e_{p,j}\epsilon_{il}) R_l \quad , \tag{2.30}$$

where $\vec{R} = \vec{r}_1 - \vec{r}_2$. Inserting this contribution into Eq. (2.17), we integrate freely over the positions of the singularities $\vec{r}_1$ and $\vec{r}_2$. Since the first and second complexions shown in Fig. 5(a) occur with probabilities

$$P_1 = y^2 (R/a)^{-K/4\pi} e^{(K/4\pi)\cos^2\theta} + O(y^4) \quad ,$$

$$P_2 = y^2 (R/a)^{-K/4\pi} e^{(K/4\pi)\sin^2\theta} + O(y^4) \quad , \tag{2.31}$$

we find that

$$C^{-1}_{R,ijkl} = C^{-1}_{ijkl} + \tfrac{1}{4}y^2 \sum_{p=1}^{2} (e_{p,i}\epsilon_{js} + e_{p,j}\epsilon_{is})(e_{p,k}\epsilon_{lt} + e_{p,l}\epsilon_{kt}) \times \int_{|\vec{R}|>a} \frac{d^2R}{a^2} \frac{R_s R_t}{a^2} A_p \left(\frac{R}{a}\right)^{-K/4\pi} + O(y^4) \ , \tag{2.32}$$

where the weight factors A_p are

$$A_1 = e^{(K/4\pi)\cos^2\theta} \ , \quad A_2 = e^{(K/4\pi)\sin^2\theta} \ . \tag{2.33}$$

The factor of area in Eq. (2.17) has been eliminated by one of the integrations over space.

Since in reality three elastic constants are needed to describe a square lattice,[7] we do not expect the renormalizations associated with a square array of Burger's vectors to preserve an initially isotropic elastic matrix. It is straightforward to check from Eq. (2.32) that the $O(y^2)$ corrections do indeed induce a cubic anisotropy in $C^{-1}_{R,ijkl}$. A consistent calculation for melting of a square array would start with a more complicated dislocation Hamiltonian $\mathcal{H}_D$ associated with this cubic symmetry.

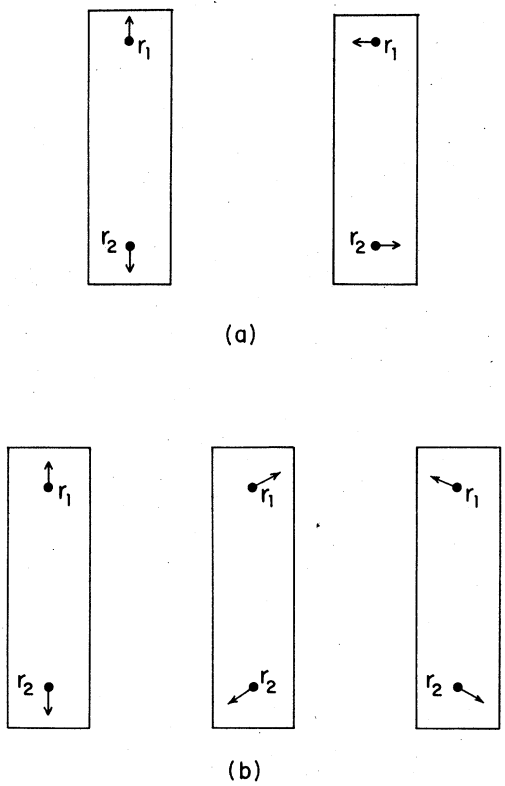

FIG. 5. Configurations of Burger's vectors at $O(y^2)$ for (a) square and (b) triangular lattices of excitations.

Fortunately, only two elastic constants are required to describe the melting of a triangular array. The relevant dislocation complexions which occur at $O(y^2)$ are shown in Fig. 5(b), the paired Burger's vectors given by $\vec{e}_p$, $p=1,2,3$, with

$$\vec{e}_1 = \begin{bmatrix} 1 \\ 0 \end{bmatrix} , \quad \vec{e}_2 = \begin{bmatrix} -\frac{1}{2} \\ \frac{1}{2}\sqrt{3} \end{bmatrix} , \quad \vec{e}_3 = \begin{bmatrix} -\frac{1}{2} \\ -\frac{1}{2}\sqrt{3} \end{bmatrix} . \tag{2.34}$$

According to Eq. (2.12), these complexions occur with probabilities

$$P_1 = y^2 \left(\frac{R}{a}\right)^{-K/4\pi} e^{(K/4\pi)\cos^2\theta} + O(y^3) \ ,$$

$$P_2 = y^2 \left(\frac{R}{a}\right)^{-K/4\pi} e^{(K/4\pi)\cos^2(\theta-2\pi/3)} + O(y^3) \ ,$$

$$P_3 = y^2 \left(\frac{R}{a}\right)^{-K/4\pi} e^{(K/4\pi)\cos^2(\theta+2\pi/3)} + O(y^3) \ , \tag{2.35}$$

where we have $\vec{R} = \vec{r}_1 - \vec{r}_2$ and we again integrate freely over $\vec{r}_1$ and $\vec{r}_2$. The $O(y^3)$ contributions to these probabilities affect the renormalization of y and will be discussed later. Since three configurations shown in Fig. 5(b) each give a contribution to U_{ij}^{sing} of the form (2.30), we have

$$C^{-1}_{R,ijkl} = C^{-1}_{ijkl} + \tfrac{1}{4}y^2 \sum_{p=1}^{3} (e_{p,i}\epsilon_{js} + e_{p,j}\epsilon_{is})(e_{p,k}\epsilon_{lt} + e_{p,l}\epsilon_{kt}) \times \int_{|\vec{R}|>a} \frac{d^2R}{a^2} \frac{R_s R_t}{a^2} A_p \left(\frac{R}{a}\right)^{-K/4\pi} + O(y^3) \ , \tag{2.36}$$

where the angular weighting factors are

$$A_1 = e^{(K/4\pi)\cos^2\theta} \ ,$$

$$A_2 = e^{(K/4\pi)\cos^2(\theta-2\pi/3)} \ ,$$

$$A_3 = e^{(K/4\pi)\cos^2(\theta+2\pi/3)} \ . \tag{2.37}$$

To extract the renormalized Lamé coefficients $\bar{\mu}_R$ and $\bar{\lambda}_R$ from Eq. (2.36), we assume that $C^{-1}_{R,ijkl}$ has the isotropic form

$$C^{-1}_{R,ijkl} = \frac{1}{4\bar{\mu}_R}(\delta_{ik}\delta_{jl} + \delta_{il}\delta_{jk}) - \frac{\bar{\lambda}_R}{4\bar{\mu}_R(\bar{\mu}_R + \bar{\lambda}_R)}\delta_{ij}\delta_{kl} \tag{2.38}$$

(it is tedious but straightforward to check that this is indeed the case), and consider various contractions of this elasticity tensor. In this way we find

$$C^{-1}_{R,ijij}=\frac{1}{\bar{\mu}_R+\bar{\lambda}_R}=\frac{1}{\bar{\mu}+\bar{\lambda}}+6\pi y^2\left[\frac{1}{2\pi}\int_0^{2\pi}d\theta\sin^2\theta\, e^{(K/4\pi)\cos^2\theta}\right]\int_a^\infty\frac{dR}{a}\left[\frac{R}{a}\right]^{3-K/4\pi}+O(y^3)\ , \tag{2.39a}$$

and

$$C^{-1}_{R,ijij}=\frac{1}{\bar{\mu}_R}+\frac{1}{2(\bar{\mu}_R+\bar{\lambda}_R)}=\frac{1}{\bar{\mu}}+\frac{1}{2(\bar{\mu}+\bar{\lambda})}+3\pi y^2\left[\frac{1}{2\pi}\int_0^{2\pi}d\theta\, e^{(K/4\pi)\cos^2\theta}\right]\int_a^\infty\frac{dR}{a}\left[\frac{R}{a}\right]^{3-K/4\pi}$$
$$+3\pi y^2\left[\frac{1}{2\pi}\int_0^{2\pi}d\theta\sin^2\theta\, e^{(K/4\pi)\cos^2\theta}\right]\int_a^\infty\frac{dR}{a}\left[\frac{R}{a}\right]^{3-K/4\pi}+O(y^3)\ . \tag{2.39b}$$

Combining Eqs. (2.39a) and (2.39b) determines the renormalization of the coupling K which enters $\mathcal{H}_D$, i.e.,

$$K_R^{-1}=\frac{1}{4}\left[\frac{1}{\bar{\mu}_R}+\frac{1}{(\bar{\mu}_R+\bar{\lambda}_R)}\right]=K^{-1}+\tfrac{3}{4}\pi y^2\left[\frac{1}{2\pi}\int_0^{2\pi}d\theta\, e^{(K/4\pi)\cos^2\theta}\right]\int_a^\infty\frac{dR}{a}\left[\frac{R}{a}\right]^{3-K/4\pi}$$
$$+\tfrac{3}{2}\pi y^2\left[\frac{1}{2\pi}\int_0^{2\pi}d\theta\sin^2\theta\, e^{(K/4\pi)\cos^2\theta}\right]\int_a^\infty\left[\frac{dR}{a}\right]\left[\frac{R}{a}\right]^{3-K/4\pi}+O(y^3)\ . \tag{2.40}$$

A consistency check is to calculate $C^{-1}_{R,xxxx}=C^{-1}_{R,yyyy}=K_R^{-1}$, which gives a result in agreement with Eqs. (2.40).

As was the case in Ref. 32, we see that perturbation theory breaks down because of infrared divergences in the integrals in Eqs. (3.39) and (3.40) as K approaches 16π. To analyze these difficulties, we proceed as in Refs. 3, 4, and 32 to break the troublesome integrations into two parts

$$\int_a^\infty\frac{dR}{a}\to\int_a^{ae^\delta}\frac{dR}{a}+\int_{ae^\delta}^\infty\frac{dR}{a} \tag{2.41}$$

with δ small. The small R portions of the integrals can then be absorbed into redefinitions of $\bar{\mu}$, $\bar{\lambda}$, and K. Upon rescaling the large R parts of the integrals so that they again range from a to ∞, we obtain series which are identical in form to Eqs. (2.39) and (2.40), but with modified couplings $\bar{\mu}'$, $\bar{\lambda}'$, K', and y'. The rescaling factors can be absorbed into a redefinition of y. Repeating this procedure many times so that the core diameter of a dislocation is effectively increased from a to ae^l, we again find series identical in form, with couplings $\bar{\mu}(l)$, $\bar{\lambda}(l)$, $K(l)$, and $y(l)$ which are the solutions of differential recursion relations. The effective rigidity modulus $\bar{\mu}^{-1}(l)$ and bulk modulus $[\bar{\lambda}(l)+\bar{\mu}(l)]^{-1}$ satisfy

$$\frac{d\bar{\mu}^{-1}(l)}{dl}=3\pi y^2(l)\, e^{K(l)/8\pi}I_0\left[\frac{K(l)}{8\pi}\right]+O(y^3)\ , \tag{2.42a}$$

$$\frac{d[\bar{\mu}(l)+\bar{\lambda}(l)]^{-1}}{dl}=3\pi y^2(l)\, e^{K(l)/8\pi}\times\left[I_0\left[\frac{K(l)}{8\pi}\right]-I_1\left[\frac{K(l)}{8\pi}\right]\right]+O(y^3)\ , \tag{2.42b}$$

where $I_0(x)$ and $I_1(x)$ are modified Bessel functions. The couplings $K(l)$ and $y(l)$ are the solutions of

$$\frac{dK^{-1}(l)}{dl}=\tfrac{3}{2}\pi y^2(l)e^{K(l)/8\pi}I_0\left[\frac{K(l)}{8\pi}\right]-\tfrac{3}{4}\pi y^2(l)e^{K(l)/8\pi}I_1\left[\frac{K(l)}{8\pi}\right]+O(y^3)\ , \tag{2.43a}$$

$$\frac{dy(l)}{dl}=\left[2-\frac{K(l)}{8\pi}\right]y(l)+O(y^2)\ . \tag{2.43b}$$

All these differential equations are subject to the initial conditions that the effective couplings reduce to the bare or unrenormalized values at $l=0$.

To determine the $O(y^2)$ contribution to Eq. (2.43b), we must consider the complexions of three dislocations located at $\vec{r}_1$, $\vec{r}_2$, and $\vec{r}_3$ shown in Figs. 6(a) and 6(b). When two of the dislocations in these figures coalesce, as shown in Fig. 6(c), the resulting configuration resembles the paired complexions shown in Fig. 5(b). Increasing the core size in such a configuration can be viewed as producing a change in the pair probabilities P_1, P_2, and P_3. For P_1, for example, we find

$$P_1=y^2(R/a)^{-K/4\pi}e^{(K/4\pi)\cos^2\theta}\times\left[1+4\pi y\left\{\frac{1}{2\pi}\int_0^{2\pi}d\phi\times\exp\left[\frac{-K}{4\pi}\cos\left(\phi-\frac{\pi}{3}\right)\cos\left(\phi+\frac{\pi}{3}\right)\right]\right\}\right.$$
$$\left.\times\int_a^{ae^\delta}\frac{dr}{a}\left[\frac{r}{a}\right]^{1-K/8\pi}+O(y^2)\right]\ , \tag{2.44}$$

with similar expressions for P_1 and P_2. In Eq. (2.44), R and θ represent the distance and orientation associated with the separation between one dislocation and the center of mass of the coalesced pair, with the Burger's vector taken to be the vector sum of the paired Burger's vectors. The variables r and ϕ refer to the vector joining this pair; their meanings are made clear in Fig. 6(d).

If one were to extend the integration in Eq. (2.44) to infinity, one would again be confronted with a divergent integral as K approached 16π. The finite correction displayed in Eq. (2.44), however, can be absorbed into an additive renormalization of y. This effect, together with the effect of rescaling the large R integrations in the perturbation series (2.39) and (2.40), gives rise to an effective dislocation probability $y(l)$ which is the solution of

$$\frac{dy(l)}{dl} = \left[2 - \frac{K(l)}{8\pi}\right] y(l) + 2\pi y^2(l) e^{K(l)/16\pi} \times I_0\left[\frac{K(l)}{8\pi}\right] + O(y^3(l)) \quad . \tag{2.45}$$

This result, together with Eqs. (2.42) and (2.43), completes our derivation of the renormalization-group equations for melting of triangular arrays.

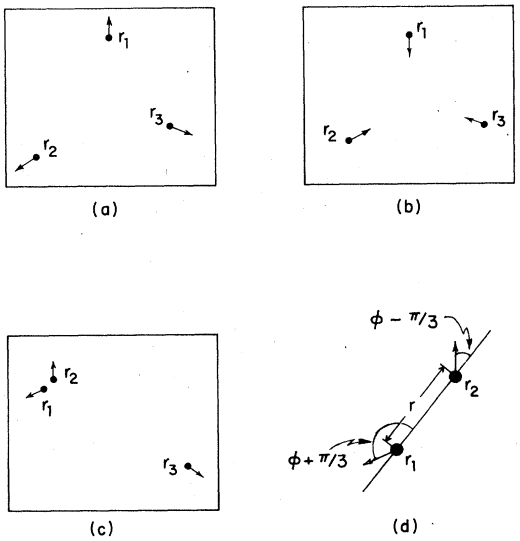

FIG. 6. Distinct triplets of Burger's vectors denoted (a) and (b) occur at $O(y^3)$. When two vectors in a triplet coalesce, as in (c), a contribution to the pair probabilities represented by Fig. 5(b) is generated. The complexion (c) renormalizes the right-hand configuration in Fig. 5(b). Part (d) is an enlargement of the region surrounding $\vec{r}$, and $\vec{r}_2$ in part (c).

III. SINGULARITIES NEAR THE MELTING TRANSITION

A. Elastic constants

An important feature of the renormalization transformation described in Sec. II B is that it preserves the form of the perturbation series for $\bar{\mu}_R$, $\bar{\lambda}_R$, and K_R. This invariance property may be written

$$\bar{\mu}_R(\bar{\mu}, \bar{\lambda}, y) = \bar{\mu}_R(\bar{\mu}(l), \bar{\lambda}(l), y(l)) \quad , \tag{3.1a}$$

$$\bar{\lambda}_R(\bar{\mu}, \bar{\lambda}, y) = \bar{\lambda}_R(\bar{\mu}(l), \bar{\lambda}(l), y(l)) \quad , \tag{3.1b}$$

$$K_R(K, y) = K_R(K(l), y(l)) \quad . \tag{3.1c}$$

The simplicity of these transformation equations (note there is no multiplicative renormalization factor) allows a convenient calculation of $\bar{\mu}_R$, $\bar{\lambda}_R$, and K. Similar results have been found in studies of compressible spin systems near four dimensions,[36] where a multiplicative renormalization factor was absorbed into a rescaling of the displacement field. In two dimensions no rescaling is necessary.

The behavior of the effective couplings $K(l)$ and $y(l)$ which appear in Eq. (3.1) is shown schematically in Fig. 7. The dislocation probability $y(l)$ tends to zero in a region to the left of the incoming separatrix, which we associate with a crystalline phase. The instability in the remaining flow trajectories towards large y signals the dissociation of dislocation pairs predicted by Kosterlitz and Thouless.[1] Although they assumed such an instability would lead to an isotropic fluid, we shall see in Sec. IV that this new phase is actually an anisotropic fluid, a liquid crystal. A typical locus of initial conditions given by Eqs. (2.13) and (2.14) is shown as a dashed line. The intersection of

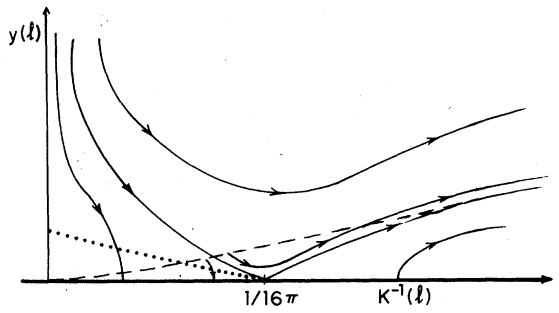

FIG. 7. Renormalization-group flows near the melting transition. The fixed line at $y(l) = 0$ is stable in the shaded region of solid phase. Quantities outside this region can be estimated by following the unstable trajectories until the correlation length is of order unity. One is then at relatively high temperatures and a simple Dubye-Hückel approximation scheme can be used. The dashed line is a typical locus of initial conditions, and the dotted line is given by $y = \frac{1}{2}m_{-}x$ (see text).

this line with the incoming separatrix determines the melting temperature T_m.

Equation (3.1) relates a potentially difficult calculation of $\bar{\mu}_R$, $\bar{\lambda}_R$, and K_R in the presence of a finite density of dislocations to one with altered couplings $K(l)$ and $y(l)$. According to Fig. 7, however, $y(l)$ tends to zero as $l \to \infty$ in the low-temperature crystalline phase. In this limit the renormalized couplings are just given by their bare values and we have from Eq. (3.1)

$$\bar{\mu}_R(\bar{\mu},\bar{\lambda},y) = \lim_{l\to\infty} \bar{\mu}(l) \ , \tag{3.2a}$$

$$\bar{\lambda}_R(\bar{\mu},\bar{\lambda},y) = \lim_{l\to\infty} \bar{\lambda}(l) \ , \tag{3.2b}$$

$$K_R(K,y) = \lim_{l\to\infty} K(l) \ . \tag{3.2c}$$

Quantities such as the Lamé coefficients can now be obtained simply by numerically integrating the recursion relations (2.42), (2.43), and (2.45). The values of $\bar{\mu}_R$ and $\bar{\lambda}_R$ obtained in this way are finite, even as $T \to T_m^-$, and of course depend on the initial conditions. We see from Fig. 7, however, that $K_R(T)$ must approach a universal constant as T approaches T_m from below

$$\lim_{T\to T_m^-} K_R(T) = \lim_{T\to T_m^-} \frac{4\bar{\mu}_R(T)[\bar{\mu}_R(T)+\bar{\lambda}_R(T)]}{2\bar{\mu}_R(T)+\bar{\lambda}_R(T)} = 16\pi \ . \tag{3.3}$$

This result is identical to the Kosterlitz-Thouless criterion for melting,[1] obtained by balancing the energy and entropy of an isolated dislocation. Recasting this equation in terms of the two-dimensional Poisson ratio $\sigma_R \equiv \lambda_R/(\lambda_R+2\mu_R)$, we find that

$$\lim_{T\to T_m^-} \bar{\mu}_R(T) = 8\pi \lim_{T\to T_m^-} [1+\sigma_R(T)]^{-1} \ , \tag{3.4}$$

which is the result claimed in the Introduction. Since we expect that $\bar{\mu}_R$ and $\bar{\lambda}_R$ are zero above T_m,[37] these quantities should be discontinuous at the melting temperature.

It is interesting to note that the renormalization-group Eq. (3.42b) produces a finite Lamé constant $\lambda_R(T)$ even if the bare value is infinite, as it would be for electrons pinned to the surface of helium.[25] This is precisely the effect one would expect dislocations to have on an otherwise incompressible lattice.

To determine how $K_R(T)$ approaches its limiting value as $T \to T_m^-$, we must study the recursion relations (2.43a) and (2.45) in more detail in the vicinity of $K = 16\pi$. To quadratic order in $y(l)$ and in a deviation $x(l)$ defined by

$$K^{-1}(l) \approx (1/16\pi)[1+x(l)] \ , \tag{3.5}$$

these equations become

$$\frac{dx(l)}{dl} = 12\pi^2 A y^2 \ , \tag{3.6a}$$

$$\frac{dy(l)}{dl} = 2xy + 2\pi B y^2 \ , \tag{3.6b}$$

where we have

$$A = 2e^2 I_0(2) - e^2 I_1(2) = 21.937\cdots \tag{3.7a}$$

$$B = e^1 I_0(2) = 6.1965\cdots \ . \tag{3.7b}$$

Equations (3.6a) and (3.6b) are structurally identical to those found for the simplified model of melting of a triangular lattice in Ref. 32. In that case, it was found that $A = B = 1$. Incoming and outgoing separatrices shown in Fig. 7 are given in the approximation (3.6) by straight-line trajectories of the form $y(l) = m_{\pm}x(l)$, with

$$m_{\pm} = (1/12\pi A)(B \pm (B^2+24A)^{1/2}) \tag{3.8}$$

As shown in Fig. 7, a Hamiltonian which starts slightly below T_m will initially hug the incoming separatrix $y = m_- x$, and then break away, plunging into the fixed line at $y = 0$. To a very good approximation the limiting value $K(l=\infty)$ will be given by $K(l^*)$, where l^* is the breakaway point defined by the condition that the trajectory cross the line $y = \frac{1}{2}m_- x$. This locus of breakaway points is shown as a dotted line in Fig. 7.

Following Ref. 32, we parametrize the trajectory of the Hamiltonian slightly below T_m by

$$y(l) = m_- x(l) + D(l) \ , \tag{3.9}$$

where the deviation $D(l)$ is initially small and proportional to $(T-T_m)/T_m \equiv t$, i.e.,

$$D(l=0) \equiv D_0 \propto -|t| \ . \tag{3.10}$$

Carrying out the analysis described in Sec. V A of Ref. 32, we find that the growth of $D(l)$ is given by

$$D(l) \approx D_0(1+12\pi^2 A m_-^2 |x_0| l)^{1/6\pi^2 A m_-^2} \ , \tag{3.11}$$

where x_0 is the negative initial value of $x(l)$. A trajectory will have broken away from the incoming separatrix when we have $l = l^*$, such that $D(l^*)$ is comparable to $m_- x(l^*)$ in Eq. (3.9). From Eq. (3.6a), however, we see that the decay of $x(l)$ to zero is given approximately by the solution of

$$\frac{dx(l)}{dl} = -12\pi^2 A m_-^2 x^2(l) \ , \tag{3.12}$$

namely,

$$x(l) = -|x_0|/(1+12\pi^2 A m_-^2 |x_0| l) \ . \tag{3.13}$$

Comparing Eq. (3.11) and (3.13), we find that breakaway occurs when we have $l = l^*$, where

$$l^* \sim |t|^{-\bar{\nu}} \tag{3.14}$$

as $t \to 0^-$, with

$$\bar{\nu} = 6\pi^2 A m_-^2/(1+6\pi^2 A m_-^2) = 0.36963477\cdots \ . \tag{3.15}$$

It now follows from Eqs. (3.5) and (3.13) that:

$$K_R^{-1} = \lim_{l\to\infty} K^{-1}(l) \approx (1/16\pi)[1+x(l^*)]$$
$$\approx (1/16\pi)(1-c|t|^{\bar{\nu}}) \ , \tag{3.16}$$

where c is a positive nonuniversal constant. The same cusplike singularity shows up in the approach of $\bar{\mu}(T)$ and $\bar{\lambda}(T)$ to their limiting values as $T \to T_m^-$.

A similar analysis may be applied to the approach of, say, $\mu_R(q, T_m^-)$ to its limiting value as q tends to zero. One finds that

$$\mu_R(q, T_m) \approx \mu_R(0, T_m^-)[1+\text{const}/\ln(qa)] \ .$$

Above T_m, we expect that μ_R tends to zero with small q, $\mu_R(q,T) \sim \xi_+^2 q^2$, where $\xi_+(T)$ is the correlation length discussed in the next subsection.

B. Correlation length and specific heat

The analysis of the correlation length and specific heat carried out for the XY model by Kosterlitz[2] and for a simplified model of melting in Ref. 32 is easily extended to the present situation. As was discussed in Sec. I, a correlation length $\xi_+(T)$ can be defined in terms of the large-distance behavior of the correlation function, i.e.,

$$C_{\vec{G}}(\vec{R}) \equiv \langle \rho_{\vec{G}}(\vec{R}) \rho_{\vec{G}}^*(\vec{0}) \rangle = \langle e^{i\vec{G}\cdot[\vec{u}(\vec{R})-\vec{u}(\vec{0})]} \rangle \ , \tag{3.17}$$

whose Fourier transform determines the structure factor $S(\vec{q})$ near $q = \vec{G}$. Although $C_{\vec{G}}(\vec{R})$ decays as a power law (see Sec. III C) in the crystalline phase, we expect that it decays exponentially for $T > T_m$, i.e.,

$$C_{\vec{G}}(\vec{R}) \sim e^{-|\vec{R}|/\xi_+(T)} \ , \tag{3.18}$$

where $\xi_+(T)$ diverges as T approaches T_m from above.

The form of this divergence follows from the way ξ_+ transforms under a renormalization-group transformation[29]

$$\xi_+(\bar{\mu}, \bar{\lambda}, y) = e^l \xi_+(\bar{\mu}(l), \bar{\lambda}(l), y(l)) \ . \tag{3.19}$$

This equation is conveniently evaluated by integrating the trajectory of a Hamiltonian initially slightly above T_m until $K^{-1}(l)$ is, say, ten percent above $1/16\pi$. At this point the correlation length on the right-hand side of Eq. (3.19) is finite, and we have

$$\xi_+(\bar{\mu}, \bar{\lambda}, y) \sim e^{l^*} \ , \tag{3.20}$$

where l^* is the "time" necessary to integrate the dislocation Hamiltonian well into the fluid phase. The relevant trajectory is shown in Fig. 7. Taking over the analysis presented in Sec. V A of Ref. 32 it can be shown from Eqs. (3.6a) and (3.6b) that l^* diverges in the same way as in Eq. (3.14) above, namely,

$$l^* \sim |t|^{-\bar{\nu}} \ , \tag{3.21}$$

where $\bar{\nu}$ is given by Eq. (3.15). Thus we have

$$\xi_+(T) \sim \exp(C/|t|^{0.36963\ldots}) \tag{3.22}$$

where C is a positive constant. If we set $A = 1$ (and $m_- = -1/3\pi$) in Eq. (3.15), we find $\bar{\nu} = \frac{2}{5}$ and $\xi_+ \sim \exp(C|t|^{-2/5})$, which are the results obtained in Ref. 32. The difference between 0.369 63... and $\frac{2}{5}$ is a measure of the importance of the angular terms in $\bar{\mathcal{H}}_D$.

The transformation law for the reduced dislocation free-energy per unit area is

$$F_D(K,y) = 6\pi\left(\frac{1}{2\pi}\int_0^{2\pi} d\theta\, e^{(K/4\pi)\cos^2\theta}\right)$$
$$\times \int_0^l e^{-2l'} y^2(l')\,dl' + e^{-2l} F_D(K(l), y(l)) \ , \tag{3.23}$$

from which it can be shown that we have

$$F_D(T) \sim e^{-2l^*} \sim \xi_+^{-2}(T) \tag{3.24}$$

near melting. Two differentiations with respect to temperature lead to a similar essential singularity in the specific heat.

C. Structure factor

The structure factor

$$S(\vec{q}) \equiv \langle \hat{\rho}(\vec{q}) \hat{\rho}^*(\vec{q}) \rangle \approx \sum_{\vec{R}} e^{i\vec{q}\cdot\vec{R}} \langle e^{i\vec{q}\cdot[\vec{u}(\vec{R})-\vec{u}(\vec{0})]} \rangle \ , \tag{3.25}$$

where the sum is over lattice sites $\vec{R}$, is of particular interest, since this quantity is probed directly by diffraction experiments on thin films.[26] We shall first discuss the solid phase, $T < T_m$.

The behavior of Eq. (3.25) for $\vec{q}$ near a reciprocal lattice vector can be determined by making a cumulant expansion,

$$C_{\vec{q}}(\vec{R}) \equiv \langle e^{i\vec{q}\cdot[\vec{u}(\vec{R})-\vec{u}(\vec{0})]} \rangle$$
$$\approx \exp\{-\tfrac{1}{2} q_i q_j$$
$$\times \langle [u_i(\vec{R}) - u_i(\vec{0})][u_j(\vec{R}) - u_j(\vec{0})] \rangle\} \ . \tag{3.26}$$

The cumulant expansion truncated at the first term as

in Eq. (3.26) is exact for the harmonic degrees of freedom $\vec{\phi}(\vec{r})$ and is correct to $O(y^2)$ for the dislocation-pair part of the displacement field. In terms of the Fourier-transformed displacement field

$$\vec{u}(\vec{q}) = \sum_{\vec{R}} e^{i\vec{q}\cdot\vec{R}} \vec{u}(\vec{R}) \ , \tag{3.27}$$

$C_q(\vec{R})$ becomes

$$C_q(\vec{R}) = \exp[q_i q_j G_{ij}'(\vec{R})] \ , \tag{3.28a}$$

with

$$G_{ij}'(\vec{R}) = \frac{1}{4\pi^2} \int d^2q \, \langle \hat{u}_i(\vec{q}) \hat{u}_j(-\vec{q}) \rangle (e^{i\vec{q}\cdot\vec{R}} - 1) \tag{3.28b}$$

and where the integration runs over the first Brillouin zone. The expectation $\langle \hat{u}_i(\vec{q}) \hat{u}_j(-\vec{q}) \rangle$ is given in the limit of small q by the renormalized elastic constants μ_R and λ_R,

$$\lim_{\vec{q}\to 0} q^2 \langle \hat{u}_i(\vec{q}) \hat{u}_j(-\vec{q}) \rangle = k_B T \left[\frac{1}{\mu_R} \delta_{ij} - \frac{\mu_R + \lambda_R}{\mu_R(2\mu_R + \lambda_R)} \frac{q_i q_j}{q^2} \right] \ . \tag{3.29}$$

This convenient alternative definition of the elastic constants was also used in Ref. 36. It is equivalent to the definition used in Sec. II. Inserting Eq. (3.29) into Eq. (3.28), we can readily extract the large $|\vec{R}|$ behavior of $G_{ij}'(\vec{R})$, i.e.,

$$G_{ij}'(\vec{R}) \approx \frac{-k_B T}{2\pi\mu_R} \frac{3\mu_R + \lambda_R}{(2\mu_R + \lambda_R)} \delta_{ij} \ln\left(\frac{|\vec{R}|}{a} \right) \ . \tag{3.30}$$

The power-law decay of $C_{\vec{G}}(\vec{R})$ then takes the form

$$C_{\vec{G}}(R) \sim 1/|\vec{R}|^{\eta_{\vec{G}}} \ , \tag{3.31}$$

with

$$\eta_{\vec{G}} = \frac{|\vec{G}|^2}{4\pi} \frac{k_B T}{\mu_R} \frac{3\mu_R + \lambda_R}{2\mu_R + \lambda_R} \ . \tag{3.32}$$

A more careful argument, which makes use of a homogeneity relation like that displayed in Eq. (3.36), reveals that there are logarithmic corrections to Eq. (3.31) precisely at T_m. Such corrections are virtually undetectable experimentally, so we will ignore them.

Inserting Eq. (3.31) into Eq. (3.25), we recover the usual power-law divergences at the Bragg points[8,12]

$$S(\vec{q}) \sim 1/|\vec{q} - \vec{G}|^{2-\eta_{\vec{G}}} \ , \tag{3.33}$$

where $\vec{G}$ is a Bragg point. Contours of constant $\eta_{\vec{G}_0}$, the exponent for the first-reciprocal lattice point (where $|\vec{G}_0|^2 = 16\pi^2/3a^2$), are shown in Fig. 8, together with the locus of melting transitions in the $\mu_R^{-1} - \sigma_R$ plane. Inserting Eq. (3.4) into Eq. (3.32), we obtain the behavior of η_{G_0} along this locus discussed in Sec. I,

$$\eta_{G_0}{}^* \equiv \lim_{T\to T_m^-} \eta_{G_0}(T) = \lim_{T\to T_m^-} \frac{1}{12}[3 - \sigma_R(T)][1 + \sigma_R(T)] \ . \tag{3.34}$$

According to Eq. (3.32), higher-order Bragg points will have larger exponents $\eta_{\vec{G}}{}^*$. When $\eta_{\vec{G}}{}^*$ exceeds 2, the infinities at the Bragg points are replaced by cusped singularities.

Because $C_G(\vec{R})$ decays exponentially above T_m, the structure factor will be finite at the Bragg points,

$$S(\vec{G}) = \sum_{\vec{R}} \langle e^{i\vec{G}\cdot[\vec{u}(\vec{R}) - \vec{u}(\vec{0})]} \rangle < \infty \ . \tag{3.35}$$

There can be divergences at these points, however as $T \to T_m^+$. It can be shown that the transformation law for $S(\vec{G})$ under the renormalization procedure of Sec. II is

$$S(\vec{G}; \bar{\mu}, \bar{\lambda}, y) = \exp\left[2l - \int_0^l \eta_{\vec{G}}(l') \, dl' \right] \times S(\vec{G}, \bar{\mu}(l), \bar{\lambda}(l), y(l)) \ , \tag{3.36}$$

where

$$\eta_{\vec{G}}(l) = \frac{|\vec{G}|^2 a_0^2}{4\pi\bar{\mu}(l)} \left(\frac{3\bar{\mu}(l) + \bar{\lambda}(l)}{2\bar{\mu}(l) + \bar{\lambda}(l)} \right) \ . \tag{3.37}$$

Evaluating the homegeneity relation at the same l^* as was used to evaluate $\xi_+(T)$, we obtain

$$S(\vec{G}; T) \sim \xi_+^{2-\eta_G{}^*} \ , \tag{3.38}$$

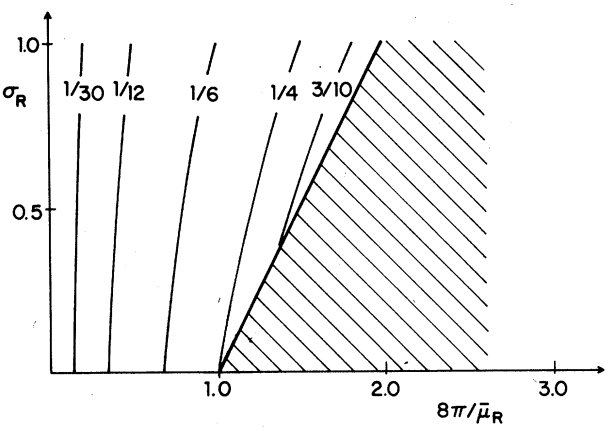

FIG. 8. Lines of constant η_{G_0} in a plane determined by Poisson's ration σ_R and the inverse reduced shear modulus $\bar{\mu}_R^{-1}$. The locus of dislocation-unbinding transitions is shown as a heavy line. Values of σ_R nd $\bar{\mu}_R^{-1}$ in the shaded region cannot occur in the solid phase. Note tht η_{G_0} never exceeds $\frac{1}{3}$, which it achieves precisely at T_m when we have $\sigma_R = 1$.

as T approaches T_m, where $\eta_G{}^*$ is given by Eq. (1.18). Since $\xi_+(T)$ diverges exponentially, peaks in $S(\vec{q})$ at the Bragg points should be a prominent feature in a diffraction experiment near T_m. Note the differing divergences at the different Bragg positions. Since the width of the peaks should be proportional to ξ_+^{-1}, the integrated intensity in any peak remains finite at T_m. Note that the integrated intensity for $|\vec{q}-\vec{G}| \lesssim \xi_+^{-1}$ is given by

$$I_l \sim \xi_+^{-2} S(\vec{G},T) \sim \xi_+^{-\eta_G^*} \quad . \tag{3.39}$$

The free dislocations present above T_m permit a shear stress to relax by the process of dislocation motion.[38] It may be seen that there will be a finite viscosity $\nu(T)$ above T_m with magnitude inversely proportional to the density n_f of free vortices, i.e.,

$$\nu(T) \propto \xi_+^2(T) \tag{3.40}$$

[Cf. the relaxation of superflow, discussed in Ref. 5.] We neglect here the weak divergence of $\nu(T)$ at long wavelengths, which is expected for any two-dimensional fluid. A more complete discussion of the dynamics near T_m will be given in a separate publication.

IV. ORIENTATIONAL ORDER AND THE DISCLINATION-UNBINDING TRANSITION

A. Orientational order below T_m

Thus far we have not discussed orientational correlations above and below T_m. As has been observed by Mermin,[11] the solid phase has long-range orientational order. Mermin noted that averages of the form

$$\langle [\vec{u}(\vec{R}+a_0\vec{e}_i)-\vec{u}(\vec{R})]\cdot[\vec{u}(a_0\vec{e}_i)-\vec{u}(\vec{0})]\rangle \quad , \tag{4.1}$$

with $i=1,2$, are nonvanishing (and are, in fact, equal to a_0^2) when evaluated using a simple harmonic theory of phonons. Clearly, this means that the angles of bonds connecting nearest neighbors are correlated over large distances even though long-range tranlational order is absent.

A closely related measure of bond correlations is the orientational order parameter $\psi(\vec{r}) = e^{6i\theta(\vec{r})}$ discussed in Sec. I. Note that a bond-angle field can be defined even in a liquid, provided a suitable definition of "nearest neighbor" is made.[39] Since $\theta(\vec{r})$ is related to the displacement field $\vec{u}(\vec{r})$ in the continuum limit by

$$\theta(\vec{r}) = \tfrac{1}{2}\epsilon_{ij}\partial_i u_j(\vec{r}) \quad , \tag{4.2}$$

it is straightforward to compute the correlation function analogous to Eq. (4.1), namely,

$$\begin{aligned}\langle \psi^*(\vec{r})\psi(\vec{0})\rangle &= \exp[-36(\langle\theta^2(\vec{0})\rangle - \langle\theta(\vec{r})\theta(\vec{0})\rangle)] \\ &= \exp\Big[-9\epsilon_{ij}\epsilon_{mn}\int_q D_{jn}^{-1}(\vec{q}) \\ &\quad \times q_i q_m (1-e^{i\vec{q}\cdot\vec{R}})\Big] \quad .\end{aligned} \tag{4.3}$$

In Eq. (4.3) $\int_q$ means $(1/4\pi^2)\int d^2q$, and $D_{jn}^{-1}(\vec{q})$ is the inverse of the dynamical matrix appropriate to isotropic continuum-elasticity theory, i.e.,

$$D_{jn}^{-1}(\vec{q}) = \frac{1}{\mu q^2}\left(\delta_{jn} - \frac{q_j q_n}{q^2}\right) + \frac{1}{2\mu+\lambda}\frac{q_j q_n}{q^4} \quad . \tag{4.4}$$

Remembering that the effect of dislocations can be absorbed in renormalized elastic constants $\mu_R(T)$ and $\lambda_R(T)$, and making use of antisymmetry of ϵ_{ij}, we find

$$\langle \psi^*(\vec{r})\psi(\vec{0})\rangle \approx \exp\left[\frac{-9k_BT}{2\pi}\int_0^\Lambda dq\, q\frac{1-J_0(qr)}{\mu_R(\vec{q},T)}\right] \quad , \tag{4.5}$$

where Λ is an appropriate ultraviolet cutoff, say, $\Lambda \sim a_0^{-1}$ and $\mu_R(\vec{q},T)$ is the wave-vector dependent shear modulus. This, of course, is a continuous function of temperature except at $\vec{q}=0$.

According to Eq. (4.5), $\langle \psi^*(\vec{r})\psi(\vec{0})\rangle$ does indeed decay to a nonvanishing value at large $\vec{r}$ given approximately by

$$|\langle\psi(\vec{r})\rangle| \approx \exp -[9k_BT\Lambda^2/8\pi\mu_R(T)] \quad . \tag{4.6}$$

The behavior of $\mu_R(T)$ and $|\langle\psi(\vec{r})\rangle$ as a function of temperature is indicated schematically in Fig. 9. Although $\mu_R(T)$ displays a $|T-T_m|^{0.36963\ldots}$ cusp as T goes to T_m from below, $|\langle\psi(\vec{r})\rangle|$ contains only an essential singularity. If Eq. (4.6) were exact, one would of course also have a cusp in $|\langle\psi(\vec{r})\rangle|$. Only the $\vec{q}=0$ component of the shear modulus $\mu_R(\vec{q},T)$ entering the more accurate formula (4.5) has this cusp, however. The small $\vec{q}$ part of the integration in Eq. (4.5) is damped out by phase-space factors, which converts the cusp in $\mu_R(\vec{0},T)$ into an essential singularity in $|\langle\psi(\vec{r})\rangle|$.

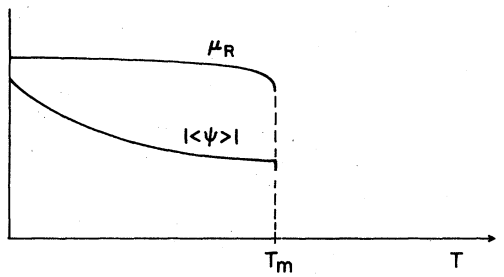

FIG. 9. Variation of the shear modulus μ_R and orientational order parameter $|\langle\psi\rangle|$ on a smooth substrate. Both quantities drop discontinuously to zero at T_m.

B. Orientational correlations above T_m

To see that $\langle \psi^*(\vec{r})\psi(\vec{0})\rangle$ tends algebraically to zero at large $\vec{r}$ just above T_m, we must determine the effect of a gas of free dislocations on orientational fluctuations. As discussed in Sec. III, the elastic constants $\mu_R(T)$ and $\lambda_R(T)$ vanish above T_m. If there is residual orientational order above T_m, we expect this will be controlled by a Hamiltonian of the form

$$\mathcal{H}_A = \tfrac{1}{2} K_A(T) \int |\vec{\nabla}\theta(\vec{r})|^2 d^2r \ , \tag{4.7}$$

where $K_A(T)$ plays the role of a Frank constant in a liquid crystal. Although K_A would be a tensor of rank two in a two-dimensional nematic,[17] the sixfold symmetry in the present case leads to a single scalar constant.

To check this hypothesis we must calculate $K_A(T)$, which is given by

$$k_B T/K_A = \lim_{q\to 0} (q^2/\Omega)\langle \hat{\theta}(\vec{q})\hat{\theta}(-\vec{q})\rangle \ , \tag{4.8}$$

where $\hat{\theta}(\vec{q})$ is the Fourier-transformed bond-angle field,

$$\hat{\theta}(\vec{q}) = \int d^2r\, e^{i\vec{q}\cdot\vec{r}}\theta(\vec{r}) \ . \tag{4.9}$$

Since it is easily seen that the smooth part of the displacement field does not contribute to Eq. (4.8), we must determine the Burger's vector contribution to $\hat{\theta}(\vec{q})$ to proceed further. According to standard texts on dislocation theory,[19] the displacement field $\vec{u}^{\,\text{sing}}(\vec{r})$ surrounding a dislocation of Burger's vector $\vec{b}$ in the $\hat{x}$ direction located at the origin is

$$u_x^{\text{sing}}(\vec{r}) = \frac{1}{2\mu}\frac{\partial\chi}{\partial x} + \frac{4}{K_0}P \ , \tag{4.10a}$$

$$u_y^{\text{sing}}(\vec{r}) = -\frac{1}{2\mu}\frac{\partial\chi}{\partial y} + \frac{4}{K_0}Q \ , \tag{4.10b}$$

where $\chi(\vec{r})$ is a function which drops out of the present calculation, and

$$P(\vec{r}) = \frac{-K_0 a_0 b}{2\pi}\tan^{-1}\left(\frac{y}{x}\right), \quad Q(\vec{r}) = \frac{K_0 a_0 b}{2\pi}\ln\left(\frac{r}{a}\right) . \tag{4.11}$$

Forming

$$\theta_s(\vec{r}) \equiv \tfrac{1}{2}[\partial_x u_y(\vec{r}) - \partial_y u_x(\vec{r})] \ ,$$

we find that the rotation induced by an isolated dislocation $\theta_s(\vec{r}) = -a_0 bx/2\pi r^2$. The generalization to an arbitrary complexion of Burger's vectors $\vec{b}(\vec{r})$ is immediate, i.e.,

$$\theta_s(\vec{r}) = \frac{-a_0}{2\pi}\sum_{\vec{r}'}\frac{\vec{b}(\vec{r}')\cdot(\vec{r}-\vec{r}')}{|\vec{r}-\vec{r}'|^2} \ . \tag{4.12}$$

Upon Fourier transformation we obtain

$$\hat{\theta}_s(\vec{q}) = [-i\vec{q}\cdot\hat{\vec{b}}(\vec{q})a_0]/q^2 \ , \tag{4.13}$$

where $\hat{\vec{b}}(\vec{q})$ is the Fourier-transformed Burger's vector field, so that

$$k_B T/K_A = \lim_{q\to 0}(a_0^2/\Omega)(q_i q_j/q^2)\langle \hat{b}_i(\vec{q})\hat{b}_j(-\vec{q})\rangle \ . \tag{4.14}$$

It is difficult to evaluate Eq. (4.14) directly just above T_m, where the physics is dominated by a mixture of free and bound dislocations. As is evident from Eq. (3.22), the correlation length in this region is quite large. This calculation can be related, however, to a more tractable one far from T_m by the renormalization equations constructed in Sec. II. This renormalization transformation was constructed to keep the renormalized elastic constants (2.16) invariant. Since Eq. (4.8) defining K_A involves two more gradients, the transformation law for K_A is simply

$$\frac{K_A}{k_B T} \equiv \bar{K}_A(\bar{\mu},\bar{\lambda},y) = e^{2l}\bar{K}_A(\bar{\mu}(l),\bar{\lambda}(l),y(l)) \tag{4.15}$$

in contrast to Eq. (3.1). We shall determine $K_A(T)$ by evaluating the right-hand side of Eq. (4.15) at the same value of $l = l^*$ we used to determine the correlation length $\xi_+(T)$ (see Fig. 7). One is left with the relatively simple high-temperature problem of determining

$$\bar{K}_A(\bar{\mu}(l^*),\bar{\lambda}(l^*),y(l^*)) \ .$$

At sufficiently high temperatures, K_A can be calculated using Debye-Huckel theory, which amounts to treating $\vec{b}(\vec{r})$ in $\mathcal{H}_D$ [see Eq. (2.12)] as a vector of continuous length. (This approximation is discussed further in Appendix B.) We shall actually treat the more general dislocation Hamiltonian (1.24) in this way. Upon Fourier transformation (see Appendix A), Eq. (1.24) becomes

$$\frac{\mathcal{H}_D}{k_B T} = \frac{1}{2}\int_q \left\{\frac{1}{q^2}\left[\frac{K_1+K_2}{2}\left(\delta_{ij}-\frac{q_i q_j}{q^2}\right)+\frac{K_1-K_2}{2}\frac{q_i q_j}{q^2}\right] + \frac{2E_c a^2}{k_B T}\delta_{ij}\right\}\hat{b}_i(\vec{q})\hat{b}_j(-\vec{q}) \ . \tag{4.16}$$

This is a small momentum approximation, designed to reproduce the large $|\vec{r}-\vec{r}'|$ behavior displayed in Eq. (1.24). A cutoff-dependent constant has been absorbed into a redefinition of the core energy.

Integrating freely over the $\hat{b}_i(\vec{q})$, it is now straightforward to evaluate the average in Eq. (4.14), i.e.,

$$\langle \hat{b}_i(\vec{q})\hat{b}_j(-\vec{q})\rangle = \frac{2q^2\Omega}{K_1+K_2+4E_c q^2 a^2/k_B T}\left(\delta_{ij}-\frac{q_i q_j}{q^2}\right) + \frac{2q^2\Omega}{K_1-K_2+4E_c q^2 a^2/k_B T}\frac{q_i q_j}{q^2} \ . \tag{4.17}$$

Since the part proportional to the transverse-projection operator does not contribute to K_a^{-1}, we obtain

$$\frac{k_BT}{K_A}=\lim_{q\to 0}\frac{2q^2}{K_1-K_2+4E_cq^2a^2/k_BT}$$
$$=\begin{cases}k_BT/2E_ca^2\ , & K_1=K_2\ ,\\ 0\ , & K_1\neq K_2\ .\end{cases} \tag{4.18}$$

For the case of a smooth substrate ($K_1=K_2$), we find $K_A\approx 2E_ca^2/a_0=O(k_BT_m)$, a finite result. Combining this with Eq. (4.15), one finally obtains

$$K_A(T)/k_BT\sim e^{2l^*}\sim\xi_+^2(T)\ . \tag{4.19a}$$

For the case $K_1\neq K_2$ (which describes melting on a periodic substrate—see Sec. V) we have

$$K_A(T)=\infty\ , \tag{4.19b}$$

indicating that true long-range orientational order persists in this case.

Having determined the Frank constant which enters Eq. (4.7), we are in a position to study the decay of orientational order. A standard[40] calculation gives

$$\langle\psi^*(\vec{r})\psi(\vec{0})\rangle\sim r^{-\eta_6(T)} \tag{4.20}$$

with

$$\eta_6(T)=18k_BT/\pi K_A(T)\ . \tag{4.21}$$

This slow decay of orientational order leads us to identify the phase above T_m as a kind of two-dimensional liquid crystal. Note that $\eta_6(T)$ tends to zero rapidly as T goes to T_m from above.

C. Disclination-unbinding transition

The algebraic decay of orientational order does not persist indefinitely, but is destroyed at a temperature $T_i>T_m$ by the dissociation of pairs of $\pm 60°$ disclinations. Indeed, the system is now isomorphic to the model of superfluidity and XY magnetism treated by Kosterlitz,[2] except that disclinations play the role of vortices. Following Kosterlitz, we decompose the bond-angle field $\theta(\vec{r})$ into smoothly varying part $\phi(\vec{r})$ and a part due to a collection of disclinations. Inserting this decomposition into Eq. (4.7), one obtains

$$\mathcal{H}_D=\tfrac{1}{2}K_A\int d^2r(\vec{\nabla}\phi)^2$$
$$-\frac{\pi K_A}{36}\sum_{\vec{r}\neq\vec{r}'}s(\vec{r})s(\vec{r}')\ln\left|\frac{\vec{r}-\vec{r}'}{a}\right|$$
$$+E_c\sum_{\vec{r}}s^2(\vec{r})\ , \tag{4.22}$$

where $s(\vec{r})=0,\ \pm 1,\ \pm 2,\ \pm 3,\ldots$ is an integer measure of the disclinicity at the point $\vec{r}$, a is the disclination core size, and E_c a disclination core energy. Note that the screening effect of a gas of dislocations has produced a rather weak logarithmic interaction between disclinations. Disclination pairs are quite tightly bound in the solid phase with energy increasing as the square of the separation.[19]

The transcription of Kosterlitz's results is immediate. A disclination-unbinding transition occurs at a temperature T_i such that we have[2]

$$\eta_6(T_i)=\tfrac{1}{4}\ . \tag{4.23}$$

In analogy to the behavior of the superfluid density in a ^{4}He film,[4] the renormalized Frank constant should jump discontinuously to zero at T_i,[41]

$$\lim_{T\to T_i^-}K_A(T)=72k_BT_i/\pi\ . \tag{4.24}$$

Above T_i, one obtains exponentially decaying orientational order in an isotropic liquid

$$\langle\psi^*(\vec{r})\psi(\vec{0})\rangle\sim e^{-r/\xi_\psi(T)}\ , \tag{4.25}$$

where the orientational correlation length $\xi_\psi(T)$ is strongly divergent. As $T\to T_i^+$, one finds[2]

$$\xi_\psi(T)\sim e^{b/|T-T_i|^{1/2}}\ , \tag{4.26}$$

where b is a constant. As usual, there is only an essential singularity in the specific heat, i.e.,

$$C_p\sim\xi_\psi^{-2}\ . \tag{4.27}$$

V. PERIODIC SUBSTRATE POTENTIALS

Since many experiments are carried out on solid-liquid transitions in films adsorbed onto a crystalline substrate,[26] it is important to determine the effect of commensurate and incommensurate periodic potentials on our results.

A. Weak incommensurate potentials

Consider a Hamiltonian of the form

$$\frac{\mathcal{H}}{k_BT}=\frac{\mathcal{H}_E}{k_BT}-\sum_{\vec{R}}V(\vec{R}+u(\vec{R}))\ , \tag{5.1}$$

where $\mathcal{H}_E$ is given by Eq. (2.1) (with dislocations included), the summation is over lattice sites of the adsorbed crystal, and $V(\vec{r})$ has the periodicity of the substrate. An overall factor $-1/k_BT$ has been absorbed into the definition of this potential. The function $V(\vec{r})$ has the Fourier representation

$$V(\vec{r}) = \sum_{\vec{K}} h_{\vec{K}} e^{i\vec{K}\cdot\vec{r}} , \tag{5.2}$$

where the sum is over the reciprocal lattice $\{\vec{K}\}$ of the substrate and

$$h_{\vec{K}} = \frac{1}{\Omega}\int d^2r\, e^{-i\vec{K}\cdot\vec{r}} V(\vec{r}) , \tag{5.3}$$

where Ω is the area of the system.

If none of the $\{\vec{K}\}$ in the sum (5.2) coincides with an adsorbate recirpocal-lattice vector, the substrate potential is incommensurate with the adsorbate lattice. Physically, one might expect that weak potentials of this kind could be neglected at long wavelengths, with some slight modification of the continuum-elastic theory appropriate to a smooth substrate. To study this further, let us expand the periodic part of Eq. (5.1) in the displacements $\vec{u}(\vec{r})$,

$$\frac{-\mathcal{H}}{k_B T} = \frac{-1}{2k_B T}\int_q \hat{u}_i(\vec{q}) D_{ij}(\vec{q}) \hat{u}_j(-\vec{q}) + \sum_{\vec{R}}\sum_{\vec{K}} h_{\vec{K}} + \sum_{\vec{R}}\sum_{\vec{K}} h_{\vec{K}} e^{i\vec{K}\cdot\vec{R}}\{1 + i\vec{K}\cdot\vec{u}(\vec{R}) + \cdots\} \tag{5.4}$$

The elastic part of the Hamiltonian $\mathcal{H}_E$ has been Fourier transformed and written in terms of the dynamical matrix $D_{ij}(\vec{q})$. Although $D_{ij}(\vec{q})$ has the usual isotropic form appropriate to a triangular lattice at small $\vec{q}$,

$$D_{ij}(\vec{q}) = \mu q^2 \delta_{ij} + (\mu+\lambda) q_i q_j + O(q^4) , \tag{5.5}$$

we shall be interested in the properties of this matrix far from $\vec{q}=0$, where the underlying lattice structure makes $D_{ij}(\vec{q})$ manifestly anisotropic. In particular, $D_{ij}(\vec{q})$ should have the periodicity of the adsorbate reciprocal lattice.

The first term in the expansion of the potential in Eq. (5.4) vanishes and the term linear in $\vec{u}(\vec{r})$ can be eliminated by a shift in $\vec{\hat{u}}(\vec{q})$, i.e.,

$$\hat{u}_i(\vec{q}) \to \hat{u}_i'(\vec{q}) = \hat{u}_i(\vec{q}) + \delta\hat{u}_i(\vec{q}) , \tag{5.6}$$

with

$$\delta\hat{u}_i(\vec{q}) = iD_{ij}^{-1}(\vec{q}) \sum_{\vec{K}} K_j h_{\vec{K}} \Delta_{\vec{K},\vec{q}} . \tag{5.7}$$

The function $\Delta_{\vec{K},\vec{q}}$ is unity if we have $\vec{K} = \vec{q} + \vec{G}$ for some adsorbate reciprocal-lattice vector $\vec{G}$, and equals zero otherwise. Inserting Eq. (5.6) into Eq. (5.4), we obtain

$$\frac{\mathcal{H}}{k_B T} = \frac{1}{2k_B T}\int_q \hat{u}_i'(\vec{q}) D_{ij}(\vec{q}) \hat{u}_j'(\vec{q}) - \frac{\Omega}{2}\sum_{\vec{K}} h_{\vec{K}}^2 K_i D_{ij}^{-1}(\vec{K}) K_j + \cdots . \tag{5.8}$$

Rewriting $D_{ij}(\vec{q})$ in terms of polarization vectors $\vec{\epsilon}_s(\vec{K})$ and eigenfrequencies $\omega_s(\vec{K})$, the second term in Eq. (5.8) becomes

$$C(\theta) \equiv -\frac{\Omega}{2}\sum_{\vec{K}}\sum_{s=1}^{2} h_{\vec{K}}^2 \frac{[\vec{K}\cdot\vec{\epsilon}_s(\vec{K})]^2}{\omega_s^2(\vec{K})} . \tag{5.9}$$

Although C is independent of the displacements, it clearly depends on the orientation angle θ of the adsorbate lattice measured from some preferred orientation relative to the substrate. The function $C(\theta)$ has sixfold symmetry for triangular adsorbates on triangular substrates, but a 12-fold symmetry for triangular adsorbates on square substrates. It has the Fourier expansions

$$C(\theta) = \Omega \sum_{j=0}^{\infty} c_j \cos(6j\theta) \tag{5.10}$$

(triangular substrate), and

$$C(\theta) = \Omega \sum_{j=0}^{\infty} c_j \cos(12j\theta) \tag{5.11}$$

(square substrate), where we take $\theta = 0$ to correspond to perfect alignment. Of course, the substrate and adsorbate crystallographic axes need not be aligned with each other in the state of minimum energy.[42] It will then be convenient, for the following discussion, to redefine θ to be measured relative to the minimum-energy orientation.

If the relative orientation of the adsorbate and substrate lattices is now allowed to vary slowly in space, θ becomes the bond angle field $\theta(\vec{r}) = \frac{1}{2}(\partial_y u_x' - \partial_x u_y')$ discussed in Sec. I. For small deviations of $\theta(\vec{r})$ from perfect alignment, the effective elastic Hamiltonian at long wavelengths is now

$$\mathcal{H}_E = \frac{1}{2}\int dr^2 [2\mu u_{ij}^2 + \lambda u_{kk}^2 + \gamma(\partial_y u_x - \partial_x u_y)^2] , \tag{5.12}$$

where we have dropped the primes on $\vec{u}$, and where $\gamma = C''/4\Omega$ is a new elastic constant. Upon resolving $\vec{u}$ into a smooth part $\vec{\phi}$ and a part due to dislocations $\vec{u}_{\text{sing}}$, Eq. (5.12) becomes

$$\frac{\mathcal{H}_E}{k_B T} = \frac{1}{2}\int \frac{d^2r}{a_0^2}[2\bar{\mu}\phi_{ij}^2 + \bar{\lambda}\phi_{kk}^2 + \bar{\gamma}(\partial_y\phi_x - \partial_x\phi_y)^2] + \frac{\mathcal{H}_D}{k_B T} , \tag{5.13}$$

where $\bar{\mu}$, $\bar{\lambda}$, and $\bar{\gamma}$ are reduced elastic constants, and $\mathcal{H}_D$ is given by Eq. (1.24) with (see Appendix C)

$$K_1 = \frac{4\bar{\mu}(\bar{\mu}+\bar{\lambda})}{2\bar{\mu}+\bar{\lambda}} + \frac{4\bar{\mu}\bar{\gamma}}{\bar{\mu}+\bar{\gamma}} ,$$
$$K_2 = \frac{4\bar{\mu}(\bar{\mu}+\bar{\lambda})}{2\bar{\mu}+\bar{\lambda}} - \frac{4\bar{\mu}\bar{\gamma}}{\bar{\mu}+\bar{\gamma}} . \tag{5.14}$$

We expect a dislocation-unbinding transition in this more general dislocation problem very similar to the

one discussed in detail in Secs. II and III. Indeed, it seems clear that the generalization of the recursion relations (2.43a) and (2.45) to this situation must take the form

$$\frac{dK_1^{-1}}{dl} = 12\pi^2 A(K_1,K_2)y^2 \ , \tag{5.15a}$$

$$\frac{dy}{dl} = \left(2 - \frac{K_1}{8\pi}\right)y + 2\pi B(K_1,K_2)y^2 \ , \tag{5.15b}$$

$$\frac{dK_2^{-1}}{dl} = C(K_1,K_2)y^2 \ , \tag{5.15c}$$

where a detailed calculation would be necessary to determine the functions A, B, and C. Recursion equations of this form would lead to qualitatively similar results to those dicussed in Sec. III, except that the exponent $\bar{\nu}$ entering the correlation length now becomes a function of the limiting value $\lim_{l\to\infty} K_2(l)$ at T_m. Clearly, the renormalized value of K_1 must be 16π at T_m. Equations of the form Eq. (5.15) have recently been derived by Young.[15]

Below T_m, $y(l)$ should be driven to zero by Eq. (5.15b); the long-wavelength properties of this floating solid phase are then given by the first term of Eq. (5.13) with suitably renormalized elastic constants $\bar{\mu}_R(T)$, $\bar{\lambda}_R(T)$, and $\bar{\gamma}_R(T)$. It is straightforward to show that the exponents $\eta_{\vec{G}}(T)$ characterizing the power-law singularities at the Bragg points $\{\vec{G}\}$ in this phase are now given by Eq. (1.5) with the replacements

$$\bar{\mu}_R(T) \to \bar{\mu}_R(T) + \bar{\gamma}_R(T) \ , \tag{5.16a}$$

$$\bar{\lambda}_R(T) \to \bar{\lambda}_R(T) - 2\bar{\gamma}_R(T) \ . \tag{5.16b}$$

The sound-propagation velocities at long wavelengths are also given by their usual expressions,[7] provided one makes these replacements. Of course, the power-law Bragg peaks in the structure function discussed above should be accompanied by a set of induced δ-function peaks at the two-dimensional reciprocal lattice $\{\vec{K}\}$ of the substrate surface, as well as induced singularities of the form $S \propto |\vec{q} - \vec{G} - \vec{K}|^{-2+\eta_{\vec{G}}}$, occurring at linear combinations of elements of $\{\vec{G}\}$ and $\{\vec{K}\}$.

The changes of the replacement (5.13) makes on the disclination-unbinding transition above T_m are more profound. As was shown in Sec. IV, the Frank constant $K_A(T)$ is infinite if $K_1 \neq K_2$, indicating that conventional long-range orientational order persists even above T_m. In particular, the elastic constant $\gamma_R(T)$ remains nonzero.

From Eq. (5.11a), we see that the effect of a triangular substrate is to produce a magnetic-field-like perturbation which couples linearly to the order parameter $\psi(\vec{r}) = e^{6i\theta(\vec{r})}$. Consequently, we expect that the disclination-unbinding transition is washed out, and that $|\langle\psi(\vec{r})\rangle|$ tends gradually to zero with increasing temperatures. For square substrates, however, Eq. (5.11b) indicates a coupling to the square of the order parameter. Since this is very similar to an Ising-like perturbation to a two-dimensional planar model,[3] we expect an Ising-like phase transition to replace the disclination unbinding present on a smooth substrate. The behavior of $|\langle\psi(\vec{r})\rangle|$ as a function of temperature in these two cases is shown in Fig. 10. A logarithmic specific heat anomaly should accompany the Ising-like phase transition on a square substrate.

B. Weak commensurate potentials

For weak substrate potentials commensurate with the adsorbate lattice they are perturbing, the adsorbate and substrate reciprocal lattices $\{\vec{G}\}$ and $\{\vec{K}\}$ have a set of wave vectors in common. The analysis presented in Sec. V A then breaks down, since some of the phonon frequencies in the denominator of Eq. (5.10) now vanish. Let $\{\vec{M}\}$ be the set of reciprocal-lattice vectors common to both $\{\vec{K}\}$ and $\{\vec{G}\}$, and let M_0 be the minimum length of the nonzero vectors in $\{\vec{M}\}$. Components of substrate potential in the expansion (5.2) not in $\{\vec{M}\}$ can be treated by the methods of Sec. V A. Terms corresponding to members of $\{\vec{M}\}$ with magnitude $|\vec{M}| > M_0$ will turn out to be more irrelevant than the terms we will consider explicitly. We are thus led to focus our attention on

$$\frac{\mathcal{H}}{k_B T} = \frac{\mathcal{H}_E}{k_B T} + \sum_{|\vec{M}|=M_0} h_{\vec{M}} \sum_{\vec{R}} e^{i\vec{M}\cdot\vec{u}(\vec{R})} \ , \tag{5.17}$$

where the effect of the incommensurate terms in Eq. (5.2) has been incorporated into $\mathcal{H}_E$.

To determine the importance of the $h_{\vec{M}}$ perturbation, we calculate its renormalization-group eigenvalue in terms of the elastic constants $\mu_R(T)$, $\lambda_R(T)$, and $\gamma_R(T)$ which appear in $\mathcal{H}_E$. We assume we are

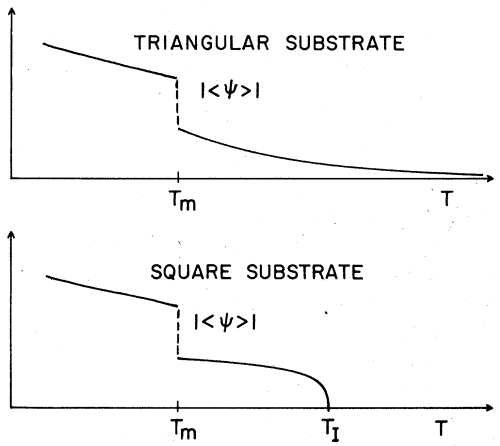

FIG. 10. Variation of the orientational order parameter for melting on triangular and square substrates.

in a floating-solid phase, and that the renormalizing effect of dislocations has already been taken into account.

Equation (5.17) takes the form

$$\frac{\mathcal{H}}{k_B T} = \frac{\mathcal{H}_E}{k_B T} + \sum_{\vec{M}-M_0} h_{\vec{M}} \sum_{\vec{R}} O_{\vec{M}}(\vec{R}) \ , \tag{5.18a}$$

with

$$O_{\vec{M}}(\vec{R}) = e^{i\vec{M}\cdot\vec{u}(\vec{R})} \ . \tag{5.18b}$$

The renormalization-group eigenvalue of $h_{\vec{M}}$ can be extracted from the large-distance behavior of autocorrelations of $O_{\vec{M}}(\vec{R})$ in the ensemble with $h_{\vec{M}}=0$. The relevant correlation function is

$$\langle O_{\vec{M}}(\vec{R}) O_{\vec{M}}^*(\vec{0})\rangle_{\mathcal{H}_E} = \langle e^{i\vec{M}\cdot[\vec{u}(\vec{r})-\vec{u}(\vec{0})]}\rangle_{\mathcal{H}_E} \sim 1/r^{\eta_{\vec{M}}} \ , \tag{5.19}$$

where

$$\eta_{\vec{M}}(T) = \frac{M_0^2 k_B T(3\mu_R+\lambda_R+\gamma_R)}{4\pi(\mu_R+\gamma_R)(2\mu_R+\lambda_R)} \ . \tag{5.20}$$

The expectation values in Eq. (5.19) are evaluated with the harmonic part of the Hamiltonian (5.13), using renormalized elastic constants.

It follows that the renormalization-group eigenvalue λ_{M_0} associated with this power-law decay is[43]

$$\lambda_{M_0} = 2 - \tfrac{1}{2}\eta_{M_0}$$
$$= 2 - \frac{M_0^2 k_B T}{8\pi(\mu_R+\gamma_R)} \frac{3\mu_R+\lambda_R+\gamma_R}{2\mu_R+\lambda_R} \ . \tag{5.21}$$

According to Eq. (5.21), all commensurate perturbations are relevant variables ($\lambda_{M_0}>0$) at sufficiently low temperatures. The strength $h_{\vec{M}}$ of these perturbations grows under repeated iterations of the renormalization transformation, presumably leading to a lattice-gas description of the absorbed film. For sufficiently coarse substrates (small M_0), λ_{M_0} remains relevant up to the temperature at which the crystal would melt in the limit $h_{\vec{M}}=0$. One now expects instead a transition directly from a low-temperature commensurate phase into a fluid, as shown for commensurate phases I and III in Fig. 4. The Kosterlitz-Thouless picture and the analysis of this paper are then inappropriate at any temperature. One could instead attempt a renormalization-group analysis of a lattice-gas model of the adsorbate, along lines taken, for example, by Berker *et al.*[28] and by Domany and Riedel.[44] The exponents associated with the transition will typically depend on the relative symmetry of the commensurate phase and underlying substrate.

For sufficiently fine substrate mesh (large M_0), commensurate perturbations will become irrelevant ($\lambda_{M_0}<0$) before dislocations cause the adsorbed film to melt. A floating solid can then exist over a finite band of temperatures, even at coverages where the adsorbate lattice happens to be commensurate with the substrate. The dotted line indicates a locus of such points, where the periodicity of the floating solid is identical to that of commensurate phase II, which occurs at lower temperatures. We expect the dislocation-unbinding transition at the point A and properties of the orientation order parameter to be as discussed in Sec. V A. The precise criterion for deciding when it is possible to have a floating solid at intermediate temperatures in the presence of a commensurate perturbation was discussed in Sec. I [see Eq. (1.23)].

C. Floating-solid commensurate transition

The floating-solid-commensurate transition can be studied in more detail at the special point marked B in Fig. 4, where the dotted line runs into commensurate phase II. This will be done by mapping this problem onto a vector Coulomb gas of the form (1.24).

Consider the Hamiltonian (5.17) well below any dislocation-unbinding temperature so that dislocations can be neglected at long wavelengths. Rather than Fourier expanding $V(\vec{R})$, as done in Eq. (5.17), let us instead represent e^V as a Fourier sum, i.e.,

$$e^{V(\vec{R}+\vec{u}(\vec{R}))} \approx \sum_{\vec{M}} A_{\vec{M}} e^{i\vec{M}\cdot\vec{u}(\vec{R})} \ , \tag{5.22}$$

where

$$A_{\vec{M}} = \frac{1}{\Omega}\int d^2r\, e^{-i\vec{M}\cdot\vec{r}+V(\vec{r})} \ . \tag{5.23}$$

Incommensurate terms in the potential have again been incorporated into $\mathcal{H}_E$. For the potentials displayed in Eq. (5.17), it is easy to show that we have

$$A_{\vec{M}} \sim \exp[-(1/2h_M)|\vec{M}|^2] \ , \tag{5.24}$$

in the limit $h_M \to 0$. More generally, let us take

$$A_{\vec{M}} = A_{\vec{0}} e^{\ln y_M |\vec{M}|^2} \ , \tag{5.25}$$

where the limit of vanishing potential strength now corresponds to $y_M \to 0$.

Inserting this decomposition into the partition sum associated with Eq. (5.17), we obtain

$$Z \equiv \mathrm{Tr} e^{-\bar{\mathcal{H}}/k_B T} \propto \sum_{\{\vec{M}(\vec{R})\}} \int D\vec{\phi}(\vec{R}) \exp\left[-\frac{1}{2}\int \frac{d^2R}{a_0^2}(\bar{\mu}_R+\bar{\gamma}_R)[\vec{\nabla}\vec{\phi}(\vec{R})]^2+(\bar{\mu}_R+\bar{\lambda}_R-\bar{\gamma}_R)[\vec{\nabla}\cdot\vec{\phi}(\vec{R})]^2 + i\int \frac{d^2R}{a_0^2}\vec{M}(\vec{R})\cdot\vec{\phi}(\vec{R}) + \ln y_M \int \frac{d^2R}{a_0^2}|\vec{M}(\vec{R})|^2\right] . \quad (5.26)$$

At each lattice site $\vec{R}$ of the adsorbed film, we sum over the reciprocal-lattice vectors $\{\vec{M}(\vec{R})\}$ of the substrate. We have approximated the elastic Hamiltonian (5.13) by

$$\frac{\bar{\mathcal{H}}_E}{k_B T} = \frac{1}{2}\int \frac{d^2r}{a_0^2}[\bar{\mu}_R(\vec{\nabla}\vec{\phi})^2+(\bar{\mu}_R+\bar{\lambda}_R)(\vec{\nabla}\cdot\vec{\phi})^2+\bar{\gamma}_R|\vec{\nabla}\times\vec{\phi}|^2]$$
$$= \frac{1}{2}\int \frac{d^2r}{a_0}[(\bar{\mu}_R+\bar{\gamma}_R)(\vec{\nabla}\vec{\phi})^2+(\bar{\mu}_R+\bar{\lambda}_R-\bar{\gamma}_R)(\vec{\nabla}\cdot\vec{\phi})^2] , \quad (5.27)$$

where $\phi(\vec{R})$ is a smoothly varying displacement field. A partition function of precisely this form was treated in Appendix A of Ref. 32 in a different context. Carrying over the manipulations described there, we integrate out the $\vec{\phi}$ field, and find

$$Z = \sum_{\{\vec{M}(\vec{R})\}}{}' \exp\left\{\int \frac{d^2R_1}{a_0^2}\int \frac{d^2R_2}{a_0^2}\left[P\vec{M}(\vec{R}_1)\cdot\vec{M}(\vec{R}_2)\ln\left(\frac{|\vec{R}_1-\vec{R}_2|}{a}\right) - Q\frac{\vec{M}(\vec{R}_1)\cdot(\vec{R}_1-\vec{R}_2)\,\vec{M}(\vec{R}_2)\cdot(\vec{R}_1-\vec{R}_2)}{|\vec{R}_1-\vec{R}_2|^2}\right] + \ln\bar{y}_M\int\frac{dR}{a_0^2}|\vec{M}(\vec{R})|^2\right\} , \quad (5.28)$$

where

$$P = \frac{k_B T(3\mu_R+\lambda_R+\gamma_R)}{4\pi(\mu_R+\gamma_R)(2\mu_R+\lambda_R)} , \quad (5.29)$$

$$Q = \frac{k_B T(\mu_R+\lambda_R-\gamma_R)}{4\pi(\mu_R+\gamma_R)(2\mu_R+\lambda_R)} , \quad (5.30)$$

and $\bar{y}_M$ is proportional to y_M, and $\sum_{\vec{R}}\vec{M}(\vec{R})=0$.

Equation (4.17) is, of course, just the vector Coulomb gas for dislocations (1.24). Note that P and Q are proportional to temperature, in contrast to the couplings K_l which appear in Eq. (1.24). Although we have not carried out a detailed renormalization-group analysis of Eq. (4.17), we expect the recursion relations for $P(l)$, $Q(l)$, and $\bar{y}_M(l)$ to have the structure (5.15), with $P=K_1$, $Q=K_2$, and $\bar{y}_M=y$. We expect in particular that $y_M(l)$ tends to zero at sufficiently high temperatures, with an instability signaling a transition into an epitaxial phase when $P\approx 4$. This transition should be very similar to the melting transition discussed in Sec. III, with an exponentially divergent correlation length as T_c is approached from the commensurate phase. A schematic plot of the expected renormalization-group flows [with the motion of $Q(l)$ suppressed] is shown in Fig. 11.

The above considerations do not apply to the floating solid-commensurate transition at points other than B in Fig. 4. Work by Luther and Pokrovsky[45] on a very simplified model of the commensurate-incommensurate transition suggests that the periodicity of the floating solid approaches that of the commensurate solid continuously, the deviation being proportional to $|T-T_c|^{1/2}$ as one approaches the transition curve at a general point. The sign of the square root changes as one passes through the point B, and of course, the square-root term vanishes precisely at B. The specific heat singularity at a general point is also stronger than at the point B.

A second possibility is that the commensurate-incommensurate transition at points other than B is first order, with a jump in the adsorbate lattice constant.

D. Strong substrate potentials

Although strong substrate potentials are difficult to treat in general, we can make some speculations based on the results of Sec. V C. Phase diagrams as a function of temperature and potential strength (at fixed coverage) are shown in Fig. 12 for both commensurate and slightly incommensurate potentials.

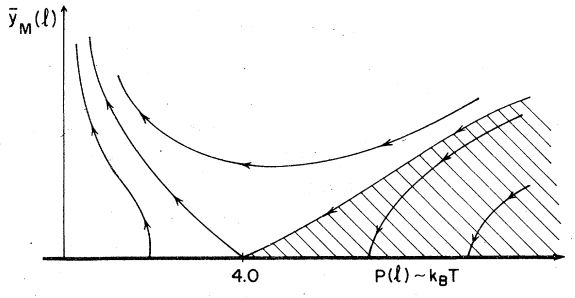

FIG. 11. Hamiltonian flows near the floating-solid–commensurate-solid phase transition. The floating solid corresponds to the shaded region, and the region of instabilities is the commensurate phase.

Fig. 12(a) shows the commensurate case for large M_0; this situation is very much like the $\cos p\theta$ perturbations treated by José *et al.*,[3] for $p > 4$. We have seen that a sufficiently weak incommensurate perturbation can be neglected at long wavelengths at all temperatures. A strong incommensurate perturbation, however, can pull an adsorbed film in partial registry, creating a new commensurate phase. This is illustrated in Fig. 12(b).

It is intriguing to consider what would happen if the three phases shown in Fig. 12 persisted even in the limit of infinite potential strength. One would then be dealing with a lattice-gas model[46] with a melting transition similar to that of a continuum model on a weak incommensurate substrate. Our results suggest that there is a critical mesh size for such lattice-gas models. Although a coarse mesh would completely obscure any continuum $d=2$ solid-fluid transitions, any mesh finer than the critical size could be used to study dislocation-unbinding transitions. The mesh in this case would cause a spurious transition into a commensurate phase at low temperatures, however, and would alter or eliminate any disclination-unbinding transition at high temperatures.

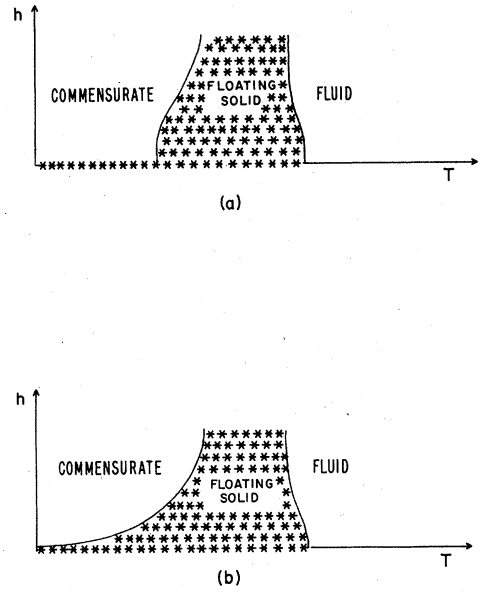

FIG. 12. (a) Phase diagram for an adsorbate subjected to a commensurate substrate perturbation with high periodicity of strength h. The line of asterisks at $h=0$ represents a solid phase on a smooth substrate. Commensurate solid, floating solid, and fluid phases exist for finite h, however. (b) Phase diagram for a slightly incommensurate potential. At any fixed temperature below melting, such potentials are unimportant for sufficiently small strengths h. Consequently a sliver of floating-solid phase extends down to zero temperature. Conversely, a sufficiently strong incommensurate potential can force the adsorbate into registry, creating a commensurate solid.

ACKNOWLEDGMENTS

It is a pleasure to acknowledge stimulating and informative conversations with A. N. Berker, R. J. Birgeneau, D. S. Fisher, A. Luther, R. Morf, L. Passel, S.-C. Ying, and A. P. Young. This work was supported in part by the NSF under Grant No. DMR 77-10210, and by the Harvard Materials Research Laboratory program. One of us (DRN) was supported by a Junior Fellowship, Harvard Society of Fellows.

write Eq. (1.24) in the form,

APPENDIX A: FOURIER REPRESENTATION OF THE DISLOCATION HAMILTONIAN

The calculations of Sec. IV make use of a Fourier representation of the dislocation Hamiltonian (1.24) valid at long wavelengths. To see that Eq. (4.16) is indeed the desired form, let us write Eq. (1.24) in the form,

$$\frac{\mathcal{H}_D}{k_B T} = -\sum_{\vec{r}_1,\vec{r}_2} V_{ij}(\vec{r}_1-\vec{r}_2)\, b_i(\vec{r}_1)\, b_j(\vec{r}_2) \ , \tag{A1}$$

and try to represent the behavior of $V_{ij}(\vec{R})$ at large $\vec{R}$ by

$$V_{ij}(\vec{R}) = \int_q \tilde{V}_{ij}(\vec{q})(1-e^{i\vec{q}\cdot\vec{R}}) \ , \tag{A2}$$

where

$$\tilde{V}_{ij}(\vec{q}) = \frac{1}{q^2}\left[X\delta_{ij} + Y\frac{q_i q_j}{q^2}\right] + Z\delta_{ij} + O\left(q^2, \frac{q_i q_j}{q^2}\right) \ . \tag{A3}$$

The integration in Eq. (A2) runs over the Brillouin zone appropriate to the lattice of possible sites for Burger's vectors, $\int_q$ means $(1/4\pi^2)\int d^2q$ and X, Y, and Z are to be determined. When inserting Eq. (A2) into Eq. (A1), the factor $(1-e^{i\vec{q}\cdot\vec{R}})$ can be replaced by $-e^{i\vec{q}\cdot\vec{R}}$, due to the charge neutrality condition $\sum_r \vec{b}(\vec{r}) = 0$.

Since Z clearly contributes only to a core energy, we concentrate on

$$V_{ij}'(R) \equiv \int_q \frac{1}{q^2}\left[X\delta_{ij} + Y\frac{q_i q_j}{q^2}\right](1-e^{i\vec{q}\cdot\vec{R}}) \ , \tag{A4}$$

which will take desired form

$$V_{ij}'(\vec{R}) \equiv \left[\frac{K_1}{8\pi}\ln\left(\frac{r}{a}\right) + C\right]\delta_{ij} - \frac{K_2}{8\pi}\frac{R_i R_j}{R^2} + O\left(\frac{a}{R}\right) \ , \tag{A5}$$

provided X and Y are chosen correctly. To extract K_1, we take the trace of Eq. (A4), perform the angular integration, and impose a convenient exponential cutoff

$$V_{kk}'(\vec{R}) = \frac{2X+Y}{2\pi}\int_0^\infty \frac{dq}{q}[1-J_0(qR)]e^{-aq} + O\left(\frac{a}{R}\right)$$
$$= \frac{2X+Y}{2\pi}\ln\left(\frac{a+(R^2+a^2)^{1/2}}{2a}\right) + O\left(\frac{a}{R}\right) . \quad \text{(A6)}$$

Comparing this with the trace of Eq. (A5), we conclude that we have

$$K_1 = 4X + 2Y \quad \text{(A7)}$$

and that $2C - K_2/8\pi$ is cutoff dependent.

Turning to the off-diagonal element of $V_{ij}'(\vec{R})$, we find

$$V_{xy}'(R) = \int_q \frac{Y}{q^2}\cos\theta\sin\theta(1-e^{iqR\cos(\theta-\phi)}) , \quad \text{(A8)}$$

where (R,ϕ) and (q,θ) are the polar coordinates of $\vec{R}$ and $\vec{q}$. Straightforward manipulations now give

$$V_{xy}'(R) = \frac{Y}{2\pi}\cos\phi\sin\phi\int_0^\infty \frac{dq}{q}J_2(qR) + O\left(\frac{a}{R}\right)$$
$$= \frac{Y}{4\pi}\cos\phi\sin\phi + O\left(\frac{a}{R}\right) . \quad \text{(A9)}$$

Comparison with Eq. (A5) now gives a cutoff independent result

$$K_2 = -2Y , \quad \text{(A10)}$$

and we conclude that the only cutoff dependence is in C. In order that Eq. (A1) agrees with Eq. (1.24), we must take

$$X = \tfrac{1}{4}(K_1+K_2) , \quad Y = -\tfrac{1}{2}K_2 . \quad \text{(A11)}$$

Substituting Eqs. (A3) and (A2) into Eq. (A1), we are led immediately to Eq. (4.16), provided Z is adjusted to give the correct core energy.

APPENDIX B: DEBYE-HÜCKEL APPROXIMATION

In this Appendix, we discuss the Debye-Hückel approximation, which was used to estimate the Frank constant $K_A(T)$ in Sec. IV. The approximation will be developed in a way which allows one to estimate the error involved in approximating sums over Burger's vectors by integrals.

We want to evaluate sums of the form

$$S = \sum_{\{\vec{b}(\vec{r})\}} \mathfrak{F}\{[\vec{b}(\vec{r})]\}\Delta\left(\sum_{\vec{r}}\vec{b}(\vec{r})\right) , \quad \text{(B1)}$$

where $\mathfrak{F}$ is some functional of a set of Burger's vectors

$$\{\vec{b}(\vec{r})\} = \{m(\vec{r})\vec{e}_1 + n(\vec{r})\vec{e}_2\}$$

located at the sites of a square lattice. The function $\Delta(\vec{x})$ is zero except at the origin, where we have $\Delta(\vec{0})=1$; it selects only those complexions of Burger's vectors which satisfy the charge neutrality condition.

At high temperatures [small K_1 and K_2 in Eq. (1.24)], dislocations with quite large Burger's vectors will be excited. This suggests that it may be reasonable to treat $\vec{b}(\vec{r})$ as a continuous vector field, rather than restricting it to the discrete points of a Bravais lattice. To make this idea precise, we apply the Poisson-summation formula[47] to each sum over $\vec{b}(\vec{r})$, making repeated use of the identity

$$\sum_{\vec{b}(\vec{r})} f(\vec{b}(\vec{r})) \equiv \sum_{m(r)=-\infty}^{\infty}\sum_{n(r)=-\infty}^{\infty} f(m(\vec{r})\vec{e}_1 + n(\vec{r})\vec{e}_2)$$
$$= \sum_{s_1(r)=-\infty}^{\infty}\sum_{s_2(r)=-\infty}^{\infty}\int_{-\infty}^{\infty} d\phi_1(\vec{r})\int_{-\infty}^{\infty} d\phi_2(\vec{r})\, f(\phi_1(\vec{r})\vec{e}_1 + \phi_2(\vec{r})\vec{e}_2)\times e^{2\pi i[s_1(\vec{r})\phi_1(\vec{r}) + s_2(\vec{r})\phi_2(\vec{r})]} \quad \text{(B2)}$$

valid for any function $f(\vec{x})$. Upon defining

$$\vec{\phi}(\vec{r}) = \phi_1(\vec{r})\vec{e}_1 + \phi_2(\vec{r})\vec{e}_2 , \quad \text{(B3)}$$

$$x = \vec{e}_1\cdot\vec{e}_2 , \quad \text{(B4)}$$

and

$$\vec{s}(\vec{r}) = s_1(\vec{r})\frac{\vec{e}_1 - x\vec{e}_2}{1-x^2} + s_2(\vec{r})\frac{x\vec{e}_1 - \vec{e}_2}{1-x^2} , \quad \text{(B5)}$$

we obtain

$$S = \sum_{\{\vec{s}(\vec{r})\}}\prod_{\vec{r}}\int d\vec{\phi}(\vec{r})\,\mathfrak{F}\{[\vec{\phi}(\vec{r})]\}\Delta\left(\sum_{\vec{r}}\phi(\vec{r})\right)$$
$$\times\exp\left[2\pi i\sum_{\vec{r}}\vec{\phi}(\vec{r})\cdot\vec{s}(\vec{r})\right] , \quad \text{(B6)}$$

where an overall factor given by the Jacobian of Eq. (B3) has been suppressed.

Setting all $\vec{s}(\vec{r})=0$, we arrive at an approximation which effectively replaces $\vec{b}(\vec{r})$ in Eq. (1.24) by a continuous vector field $\vec{\phi}(\vec{r})$. Corrections to this approximation may be found by systematically taking into account larger and larger values of the $\{\vec{s}(\vec{r})\}$. Re-expressing F in terms of

$$\hat{\phi}_i(\vec{q}) \equiv \sum_{\vec{r}} e^{i\vec{q}\cdot\vec{r}}\phi_i(\vec{r}) \quad , \tag{B7}$$

we have

$$S = \prod_{\vec{q}} \int d\hat{\phi}_i(\vec{q})\mathcal{F}\{[\hat{\phi}_i(\vec{q})]\}\Delta(\hat{\phi}_i(\vec{q}=0)) + \ldots \quad , \tag{B8}$$

where only the term corresponding to all the $\vec{s}(\vec{r})=0$ has been displayed. Using this approximation to evaluate $\langle b_i(\vec{q})b_j(\vec{q})\rangle$, we arrive immediately at Eq. (4.17). The charge conservation constraint plays no role since its only effect in Eq. (B8) is to force $\hat{\phi}_i(\vec{q}=0)$ to zero. The neglected terms in Eq. (B8) are also easy to calculate; it is straightforward to show that they are indeed negligible at high temperatures.

APPENDIX C: DISLOCATION HAMILTONIAN FOR A TRIANGULAR LATTICE ON A SIXFOLD SUBSTRATE

In Sec. V, we showed that the elastic properties of a triangular adsorbate solid could be represented by a Hamiltonian of the form

$$\mathcal{H} = \tfrac{1}{2}\int d^2r\,[2\mu u_{ij}^2 + \lambda u_{kk}^2 + \gamma(\partial_x u_y - \partial_y u_x)^2] \quad , \tag{C1}$$

where the final term arises from the preferred orientation relative to the substrate. It was argued that this would be an appropriate long-wavelength description of the elastic properties in the floating solid phase. Here, we determine the dislocation Hamiltonian corresponding to Eq. (C1).

Consider an array of dislocations, in a crystal of large but finite size. The integration in Eq. (C1) shall be taken over the area of the crystal, excluding a core region of radius a about each dislocation. The displacement $\vec{u}$ must be continuous and differentiable within the region of integration, but may be a multiple valued function, however, when dislocations are present. Specifically, the net change in $\vec{u}$ around any closed contour is the sum of the Burger's vectors of the dislocations enclosed by the contour. Our aim here is to determine the displacement $\vec{u}(\vec{r})$ which minimizes the energy (C1), for a given assignment of Burger's vectors, and to calculate the value of that energy.

The condition that the energy of a particular configuration of displacements $\vec{u}(\vec{r})$ be a minimum, with respect to small variations $\delta\vec{u}(\vec{r})$, implies that in the interior of the region of integration we have

$$\partial_i \pi_{ij} = 0 \quad , \tag{C2}$$

where $\pi_{ij}(\vec{r})$ is an asymmetric stress tensor, i.e.,

$$\pi_{ij} = 2\mu u_{ij} + \lambda u_{kk}\delta_{ij} + \gamma\epsilon_{mn}\partial_m u_n \epsilon_{ij} \quad . \tag{C3}$$

Furthermore, the normal component of π_{ij} must vanish at the boundaries, including the perimeter of the excluded core about each dislocation. It is convenient to introduce a symmetric stress tensor

$$p_{ij} = (2\mu + 2\gamma)u_{ij} + (\lambda - 2\gamma)u_{kk}\delta_{ij} \quad , \tag{C4}$$

for which it can easily be shown that in the interior, we have

$$\partial_i p_{ij} = \partial_i \pi_{ij} = 0 \quad . \tag{C5}$$

Since the equation $\partial_i p_{ij}=0$ is identical to the equation appropriate to an isotropic solid with effective elastic constants,

$$\tilde{\mu} = \mu + \gamma \quad , \quad \tilde{\lambda} = \lambda - 2\gamma \tag{C6}$$

we can take over with some important modifications, results from isotropic continuum-elasticity theory.[19]

Following the usual methods for determining the stress field surrounding a dislocation, we write the symmetric stress tensor in terms of a scalar function $\chi(\vec{r})$, i.e.,

$$p_{ij}(\vec{r}) = \epsilon_{im}\epsilon_{jn}\partial_m\partial_n\chi(\vec{r}) \quad . \tag{C7}$$

Although $p_{ij}(\vec{r})$ now automatically satisfies Eq. (C5), there are compatibility conditions which require[7,19]

$$\nabla^4\chi(\vec{r}) = 0 \quad . \tag{C8}$$

The general solution of Eq. (C8) is

$$\chi = xP + yQ + R \quad , \tag{C9}$$

where P, Q, and R are harmonic, and P and Q are harmonic conjugates. The displacements associated with a particular solution are[19]

$$u_x = \frac{-1}{2\tilde{\mu}}\frac{\partial\chi}{\partial x} + \frac{2\tilde{\mu}+\tilde{\lambda}}{\tilde{\mu}(\tilde{\mu}+\tilde{\lambda})}P \quad , \tag{C10a}$$

$$u_y = \frac{-1}{2\tilde{\mu}}\frac{\partial\chi}{\partial y} + \frac{2\tilde{\mu}+\tilde{\lambda}}{\tilde{\mu}(\tilde{\mu}+\tilde{\lambda})}Q \quad . \tag{C10b}$$

Let us try to find a solution corresponding to a dislocation at the origin, with a Burger's vector of length b in the x direction. We write

$$\chi = 2Ay\ln(r/a) + 2Bx\theta \quad , \tag{C11a}$$

$$P = (B-A)\theta \quad , \tag{C11b}$$

$$Q = (A-B)\ln(r/a) \quad , \tag{C11c}$$

where A and B are to be determined, and

$$r = (x^2+y^2)^{1/2} \quad , \quad \theta = \tan^{-1}(y/x) \quad . \tag{C12}$$

It is easily checked that χ, P, and Q are related as in Eq. (C9). The usual solution for dislocations with $\gamma=0$ corresponds to Eq. (C11) with $B=0$. To find A and B in the present case, we first require that we have

$$\oint du_x = ba_0 \ , \tag{C13a}$$

$$\oint du_y = 0 \ , \tag{C13b}$$

which leads to the condition

$$\frac{-2\pi B}{\mu+\gamma} + \frac{2\pi(\lambda+2\mu)}{(\mu+\gamma)(\mu+\lambda-\gamma)}(B-A) = ba_0 \ . \tag{C14}$$

In order for the energy to be a minimum with respect to a variation $\delta\vec{u}$ of the displacement at the perimeter of the dislocation core, we require that the net force acting across any closed circuit surrounding the dislocation vanish.[19] This force must be calculated from the asymmetric stress tensor $\pi_{ij}(\vec{r})$. Noting that we have

$$u_{ij} = (1/2\tilde{\mu})p_{ij} - [\tilde{\lambda}/4\tilde{\mu}(\tilde{\mu}+\tilde{\lambda})]p_{kk}\delta_{ij} \ , \tag{C15}$$

and using Eq. (C7), we have

$$\pi_{ij} = (\mu/\tilde{\mu})\epsilon_{im}\epsilon_{jn}\partial_m\partial_n\chi + [(\lambda\tilde{\mu}-\tilde{\lambda}\mu)/2\tilde{\mu}(\tilde{\mu}+\tilde{\lambda})] \times \nabla^2\chi\delta_{ij} + \gamma\epsilon_{mn}\partial_m u_n \epsilon_{ij} \ . \tag{C16}$$

The force F_i acting across a closed circuit, given by

$$F_i = \oint \pi_{ij} n_i \, dl \ , \tag{C17}$$

where n_i is an inwardly directed normal, can now be found using the results

$$\nabla^2\chi = 4(A-B)y/r^2 \ , \tag{C18}$$

$$\epsilon_{ij}\partial_i u_j = \frac{a_0(2\mu+\lambda)(A-B)}{(\mu+\gamma)(\mu+\lambda-\gamma)}\frac{2x}{r^2} \ . \tag{C19}$$

The force in the x direction trivially vanishes, and the force in the y direction will vanish, provided

$$\frac{\mu}{\mu+\gamma}4\pi B - \frac{4\pi\gamma(2\mu+\lambda)}{(\mu+\gamma)(\mu+\lambda-\gamma)}(A-B) = 0 \ . \tag{C20}$$

Solving Eqs. (C14) and (C21) for A and B, we finally have

$$A = -\frac{ba_0}{2\pi}\frac{(\mu+\gamma)(\mu+\lambda)}{2\mu+\lambda} \ , \quad B = \frac{-ba_0\gamma}{2\pi} \ , \tag{C21}$$

which reduces to the usual result[19] when we have $\gamma=0$.

The elastic energy of an arbitrary complexion of dislocations with displacements given by Eqs. (C11) and (C21) can be determined by the following trick. Let us differentiate the dislocation contribution to Eq. (C1) with respect to γ, i.e.,

$$\frac{\partial\mathcal{H}_D}{\partial\gamma} = \tfrac{1}{2}\int d^2r(\epsilon_{ij}\partial_i u_j)^2 + \int \frac{\delta\mathcal{H}_D}{\delta u_i}\frac{\partial u_i}{\partial\gamma}\,d^2r \ , \tag{C22}$$

where $u_i(\vec{r})$ is the displacement field due to a set of dislocations. Since we have already minimized $\mathcal{H}_D$ with respect to $\delta\vec{u}$, the second term vanishes and we are left with the comparatively simple task of evaluating the squared integral of

$$\epsilon_{ij}\partial_i u_j(\vec{r}) = \frac{-a_0}{\pi}\frac{\mu}{\mu+\gamma}\sum_{\vec{r}'}\frac{\vec{b}(\vec{r}')\cdot(\vec{r}-\vec{r}')}{|\vec{r}-\vec{r}'|^2} \ . \tag{C23}$$

This is the generalization of Eq. (C19) to an arbitrary complexion of Burger's vectors. Inserting Eq. (C23) into Eq. (C22), it can be shown after some manipulation that we have

$$\frac{\partial\mathcal{H}_D}{\partial\gamma} = \frac{2a_0^2\mu^2}{(\mu+\gamma)^2}\sum_{\vec{r}_1,\vec{r}_2} b_i(\vec{r}_1)b_j(\vec{r}_2)V_{ij}^{(2)}(\vec{r}_1-\vec{r}_2) \ , \tag{C24}$$

with

$$V_{ij}^{(2)}(\vec{r}) = \int_q \frac{q_i q_j}{q^4}(1-e^{i\vec{q}\cdot\vec{r}}) \ , \tag{C25}$$

where we have made use of the charge neutrality condition. Equation (C25) is just a special case of the quantity (A2) evaluated in Appendix A. Taking over the results tabulated there, we find

$$\frac{\partial\mathcal{H}}{\partial\gamma} = \frac{a_0^2\mu^2}{\pi(\mu+\gamma)^2}\sum_{\vec{r}\neq\vec{r}'}\left[\vec{b}(\vec{r})\cdot\vec{b}(\vec{r}')\ln\left(\frac{|\vec{r}-\vec{r}'|}{a}\right) + \frac{\vec{b}(\vec{r})\cdot(\vec{r}-\vec{r}')\,\vec{b}(\vec{r}')\cdot(\vec{r}-\vec{r}')}{|\vec{r}-\vec{r}'|^2}\right] \ , \tag{C26}$$

where a contribution to the core energy has again been suppressed.

Comparing Eq. (C26) with the γ derivative of the expected result (1.24) and going over to reduced elastic constants ($\bar{\mu}=\mu a_0^2/k_bT$, etc.), we arrive at partial-differential equations for K_1 and K_2, i.e.,

$$\frac{\partial K_1}{\partial \bar{\gamma}}=\frac{4\bar{\mu}^2}{(\bar{\mu}+\bar{\gamma})^2}\ ,\quad \frac{\partial K_2}{\partial \bar{\gamma}}=\frac{-4\bar{\mu}^2}{(\bar{\mu}+\bar{\gamma})^2}\ . \tag{C27}$$

Thus, K_1 and K_2 must have the form

$$K_1=f_1(\bar{\mu},\bar{\lambda})-\frac{4\bar{\mu}^2}{\bar{\mu}+\bar{\gamma}}\ ,$$

$$K_2=f_2(\bar{\mu},\bar{\lambda})+\frac{4\bar{\mu}^2}{\bar{\mu}+\bar{\gamma}}\ . \tag{C28}$$

Imposing the requirement that we have

$$K_1(\bar{\mu},\bar{\lambda},\bar{\gamma})|_{\bar{\gamma}=0}=K_2(\bar{\mu},\bar{\lambda},\bar{\gamma})|_{\bar{\gamma}=0}=\frac{4\bar{\mu}(\bar{\mu}+\bar{\lambda})}{2\bar{\mu}+\bar{\lambda}}\ , \tag{C29}$$

we determine f_1 and f_2, and arrive at our final results, namely,

$$K_1=\frac{4\bar{\mu}(\bar{\mu}+\bar{\lambda})}{2\bar{\mu}+\bar{\lambda}}+\frac{4\bar{\mu}\bar{\gamma}}{\bar{\mu}+\bar{\gamma}}\ ,$$

$$K_2=\frac{4\bar{\mu}(\bar{\mu}+\bar{\lambda})}{2\bar{\mu}+\bar{\lambda}}-\frac{4\bar{\mu}\bar{\gamma}}{\bar{\mu}+\bar{\gamma}}\ . \tag{C30}$$

[1]J. M. Kosterlitz and D. J. Thouless, J. Phys. C 6, 1181 (1973); Prog. Low Temp Phys. (to be published); see also, V. L. Berezinskii, Zh. Eksp. Teor. Fiz. 59, (1970) [Sov. Phys. JETP 32, 493 (1971)].

[2]J. M. Kosterlitz, J. Phys. C 7, 1046 (1974).

[3]J. José, L. P. Kadanoff, S. Kirkpatrick, and D. R. Nelson, Phys. Rev. B 16, 1217 (1977).

[4]D. R. Nelson and J. M. Kosterlitz, Phys. Rev. Lett. 39, 1201 (1977).

[5]V. Ambegaokar, B. I. Halperin, D. R. Nelson, and E. D. Siggia, Phys. Rev. Lett. 40, 783 (1978); see also B. A. Huberman, R. J. Meyerson, and S. Doniach, 40, 780 (1978); and R. J. Meyerson, Phys. Rev. B 18, 3204 (1978).

[6]B. I. Halperin and D. R. Nelson, Phys. Rev. Lett. 41, 121 (1978); E 41, 519 (1978).

[7]L. D. Landau and E. M. Lifshitz, *Theory of Elasticity* (Pergamon, New York, 1970).

[8]B. Jancovici, Phys. Rev. Lett. 19, 20 (1967); we find a dislocation unbinding transition at temperatures well below the transition temperature studied by Jancovici.

[9]R. E. Peierls, Ann. Inst. Henri Poincaré 5, 177 (1935).

[10]L. D. Landau, Phys. Z. Sowjetunion II, 26 (1937).

[11]N. D. Mermin, Phys. Rev. 176, 250 (1968).

[12]The properties of the two-dimensional harmonic solid studied by Jancovici (Ref. 8) have been explored in more detail by, e.g., H. J. Mikeska, and H. Schmidt, J. Low Temp. Phys. 2, 371 (1970); and Y. Imry and L. Gunther, Phys. Rev. B 3, 3939 (1971). Although these authors consider a theory of harmonic phonons on a lattice, it is straightforward to repeat the calculations in the language of continuum-elasticity theory, as is done here.

[13]See, e.g., H. E. Stanley, *Introduction to Phase Transitions and Critical Phenomena,* (Oxford University, New York, 1971).

[14]See also, L. D. Landau and E. M. Lifshitz, *Statistical Physics,* (Addison-Wesley, Reading, Mass., 1969), p. 466.

[15]This result has also been obtained by A. P. Young, Phys. Rev. B 19, 1855 (1979). The result for $\bar{\nu}$ originally quoted in Ref. 6 was incorrect, and was corrected in the erratum after being brought to our attention by Dr. Young.

[16]P. G. de Gennes, *The Physics of Liquid Crytsals,* (Oxford University, London, 1974), p. 111.

[17]D. R. Nelson and R. A. Pelcovits, Phys. Rev. B 16, 2191 (1977).

[18]For a discussion of two-dimensional Poisson ratios and compressibilities, see, e.g., G. A. Stewart, Phys. A 10, 671 (1974).

[19]F. R. N. Nabarro, *Theory of Dislocations,* (Clarendon, Oxford, 1967).

[20]It is intriguing to speculate that something of this kind may occur in three-dimensional melting.

[21]B. J. Alder and T. E. Wainwright, Phys. Rev. 127, 359 (1962).

[22]R. Pindak, R. Meyer, and N. A. Clark have prepared free standing films of several materials which show the smectic-*A* to smectic-*B* transition. Pindak and D. E. Moncton are currently studying these films with x-ray scattering techniques; R. Pindak and D. E. Moncton, (private communcation).

[23]R. J. Birgeneau and J. D. Litster, J. Phys. Lett. (Paris) 39, L399 (1978).

[24]P. M. Platzman and H. Fukuyama, Phys. Rev. B 10, 3150 (1974); R. W. Hockney and T. R. Brown, J. Phys. C 8, 1813 (1975); R. C. Gann, S. Chakravarty, and G. V. Chester (unpublished); C. C. Grimes and G. Adams, (unpublished).

[25]D. J. Thouless, J. Phys. C 11, L189 (1978).

[26]J. G. Dash, *Films on Solid Surfaces,* (Academic, New York, 1975).

[27]J. K. Kjems, L. Passell, H. Taub, J. G. Dash, and A. D. Novaco, Phys. Rev. B 13, 1446 (1976), see especially Fig. 8.

[28]See, e.g., A. N. Berker, S. Ostlund, and F. A. Putnam, Phys. Rev. B 17, 3650 (1978).

[29]K. G. Wilson and J. Kogut, Phys. Rev. C 12, 77 (1974).

[30]R. L. Elgin and D. L. Goodstein, Phys. Rev. A 9, 2657 (1974). These authors report that R. P. Feynman has also considered a theory of dislocation-mediated melting in two dimensions.

[31]H. Taub, K. Carneiro, J. K. Kjems, L. Passell, and J. P. McTague, Phys. Rev. B 16, 4551 (1977).

[32]D. R. Nelson, Phys. Rev. B 18, 2318 (1978).

[33]The sign of the angular or dot-product term in Eq. (2.12) is very important. It is given incorrectly in many places in the literature, including in the second part of Ref. 1. We

are grateful to A. P. Young for discussions on this point.

[34]See, e.g., A. I. Larkin and S. A. Pikin, Sov. Phys. JETP 29, 891 (1969); J. Sak, Phys. Rev. B 10, 3957 (1974).

[35]See, e.g., P. W. Anderson, Rev. Mod. Phys. 38, 298 (1966).

[36]D. J. Bergman and B. I. Halperin, Phys. Rev. B 13, 2145 (1976).

[37]It should be emphasized that the compressibility of the system remains finite and *continuous* as one passes through T_m, despite the fact that the Lamé constants μ_R and λ_R vanish above T_c. In a perfect solid at low temperatures, there is a simple relation $B = \mu + \lambda$ between the two-dimensional bulk modulus B and the Lamé coefficients of the lattice. Near the melting temperature, however, where there is a finite concentration of vacancies and interstitials (represented in the current paper by tightly bound dislocation pairs of appropriate orientation), a local dilation fluctuation in the lattice will tend to be accompanied by a change in the concentrations of vacancies and interstitials (polarization of dislocation pairs) which reduces the associated change in the particle density. One thus finds an inequality $B > \mu_R + \lambda_R$. We expect that B will have the same essential singularity as the singular part of the specific heat, $(B^{-1})_{\text{sing}} \propto [dT_c(p)/dp]^2 C_p^{\text{sing}}$, where p is the pressure. The distinction between lattice dilation and density change has been emphasized in the context of the hydrodynamic theory of solids by P. C. Martin, O. Parodi, and P. S. Pershan, Phys. Rev. A 6, 2401 (1972).

[38]W. Shockley, in *L'État Solid,* Proceedings of the Neuvième Conseil de Physique, Institute International de Physique Solvay, (R. Stoops, Bruxelles, 1952).

[39]R. Collins, *Phase Transitions and Critical Phenomena,* edited by C. Domb and M. S. Green (Academic, New York, 1972), Vol. 2, p. 271.

[40]See, e.g., F. Wegner, Z. Phys. 206, 465 (1967).

[41]The analogous prediction for nematics was given incorrectly in Ref. 4; see D. Stein, Phys. Rev. B 18, 2397 (1978).

[42]A. D. Novaco and J. P. McTague, Phys. Rev. Lett. 38, 1286 (1977).

[43]L. P. Kadanoff, *Proceedings of the Enrico Fermi Summer School of Physics, Varenna, 1970,* edited by M. S. Green (Academic, New York, 1971). A very similar calculation is given in Appendix B of Ref. 32.

[44]E. Domany and E. K. Riedel, Phys. Rev. Lett. 40, 561 (1978).

[45]A. Luther and V. L. Pokrovsky (unpublished), see also V. L. Pokrovsky and A. L. Talapor, Phys. Rev. Lett. 42, 65 (1979).

[46]Lattice gas models of melting have been reviewed by L. K. Runnels, *Phase Transitions and Critical Phenomena,* edited by C. Domb and M. S. Green, (Academic, New York, 1972), Vol. 2.

[47]See, e.g., I. M. Gel'fand and G. E. Shilov, *Generalized Functions,* (Academic, New York, 1964), Vol. 1, p. 332.